16th Symposium of AER on VVER Reactor Physics and Safety, Bratislava, Slovakia,
25 – 29 September, 2006

ON THE METHOD OF MOVING OF INCOMPLETE COOLANT MIXING CORRECTION IN THE TOP NOZZLE OF VVER-440 ASSEMBLY. CORRECTION OF POWER ASSEMBLIES USING THERMOCOUPLES READINGS

A. Brik, D. Oleksiuk.
RRC "Kurchatov Institute", Moscow, Russia

ABSTRACT

In the RRC "Kurchatov Institute" during 3 last years it was realized work package directed to development of the method of power assemblies correction using thermocouples readings.

This entire works include the experimental and calculation ones. The main result of the experiment investigations is fact of incomplete coolant mixing in the head of VVER-440 assembly. Furthermore experimental data were used for validation of CFD code PHOENICS and modernized subchannel code SC-1 (SC-1 is analogue of COBRA-IV code).

Modernized SC-1 code is capable to calculate the coolant temperature distribution in not only the fuel part of assembly but the head of assembly too.

In the future the modernized SC-1 code was used for calculation analysis of the thermocouples data that were obtained from 3-d and 4-th units of the Kola NPP.

At the results of this analysis were developed the method of the moving of incomplete coolant mixing correction in the nozzle of VVER-440 assembly.

The developed corrective functions were used for compare of calculated and measured relative assemblies power using thermocouples readings.

The main result of such comparison is that the differences between calculated and measured relative assembly powers for representative sample are reduced as a whole. Total amount of the considered variants were more than 1200 (different units, campaigns, assemblies and time moments).

INTRODUCTION

Lately in some VVER-440 reactor operating countries many calculations of the coolant flow velocity and temperature fields in the region from the fuel rod bundle to the fuel assembly (FA) thermocouple location in the channel of shield tubes (ST) have been carried out using different CFD codes [1-5]. The purpose of all the calculations was generally the same – to determine how the coolant temperature measured by the thermocouple can differ from its average mixed value at the fuel rod bundle outlet, which admittedly characterizes the fuel assembly power.

The results obtained by different specialists could be quite different. In some cases the difference of the calculated thermocouple readings could exceed the average mixed

temperature at the outlet of fuel rod bundle by 5-6^{o}C, which can amount to 15-20% of coolant heating in the fuel assembly.

This led to arising of justifiable concern about the quality of thermocontrol at the VVER-440 reactors. The problem was also complicated by the fact that the VVER-440 cores contain relatively small amount of measuring channels with self-powered neutron detectors (SPND) (36 channels per 349 fuel assemblies). The insufficient reliability of thermocouple readings could not be covered by the neutron detectors (SPND) at it is in the VVER-1000 reactors.

In the period 2005-2006 in the RRC KI critical heat flux test facility KS experimental studies on measuring the coolant temperature fields at the fuel rod bundle outlet and at the thermocouple location had been carried out. The experiments were performed using the full-scale model of second generation fuel assembly.

Now these fuel assemblies are installed in the Kola NPP-3 and NPP-4, Dukovany NPP, Bohunice and Mochovce NPPs.

The organization and method of experiments and a brief discussion of the first series of measurement results were presented in paper [6].

The results of the experiments were processed using the CFD code PHOENICS [7] and the modernized version of SC-1 code [8]. The calculation analysis of the experimental data can be considered as the validation of PHOENICS and SC-1 codes. The results of comparison should be admitted as reasonable. The maximum differences between the measured and calculated temperatures over the whole region considered do not exceed 1÷1.5^{o}C and are not higher than 0.5^{o}C at the location of the permanent thermocouple. The PHOENICS and SC-1 calculation results practically coincide.

The main conclusion of the proper experimental studies should be considered as an experimentally ascertained fact of incomplete coolant mixing in the region from the fuel bundle to the FA thermocouple installed in the ST channel.

Since the PHOENICS calculations take the time dozens of times longer than the SC-1 code ones, all further calculations of temperature fields in the fuel assemblies for the purpose of comparison with the reactor measurement data and development of correction dependences were performed using the modernized version of SC-1 code.

The purpose of the work was elaboration of method for accounting the influence of incomplete coolant mixing in the fuel assembly on readings of VVER-440 FA thermocouples.

1. STATISTICAL ANALYSIS OF MEASUREMENT DATA

Elaboration of the method of accounting for incomplete coolant mixing in determining the fuel assembly powers by the thermocontrol data was carried out basing on the analysis of measured and calculated values of coolant temperature at the fuel assemblies outlet as well as on the comparison of calculated and measured fuel assembly powers. Only reliable data of working measurements had to be used. Therefore first the statistical analysis of measurement data was made, and by the results obtained the unreliable readings of thermocouples were rejected.

1.1 INITIAL CONDITIONS AND VARIANTS

For the investigations the 19th and 20th fuel loadings as well as the 17th and 18th fuel loadings of the Kola NPP-3 and NPP-4, respectively, were chosen. The Kola NPP-3 loadings

contain the fuel assemblies with Gd-2 fuel and FAs of the first generation with cover size 143 mm and 145 mm. The Kola NPP-4 loadings are composed of fuel assemblies with Gd-1 fuel and FAs of first generation with cover size 143 mm and 145 mm.

The analysis was based on the data of working measurements obtained from the operating power units. The representativeness of the analysis was increased due to employing the symmetry property of fuel loadings. The steady states of the reactor at nominal and near-nominal power at different times of the core life were considered.

1.2 ANALYSIS TECHNIQUE OF MEASUREMENT ERRORS

The analysis was performed with the help of a specially developed code of statistical processing of the results, which permit different FA groups to be analyzed, measurement errors characteristics of these groups to be assessed and the character of error distribution to be determined.

The fuel assemblies constituting the core were divided into the symmetry groups (samples). The differences in the multiplying properties, material and geometric characteristics of the FA of the same type were supposed to be of random character. The individual error of the measurements of coolant temperature at the FAs outlet in each such group can be estimated by the formula

$$\Delta T_{mes}^{i,j} = \sum_{i=1}^{M_j} (T_{mes}^{i} - T_{av}^{j}) / T_{av}^{j} . \qquad (1.1)$$

Here T_{mes}^{i} and $T_{av}^{j} = \sum_{i=1}^{M_j} T_{mes}^{i} / M_j$, the coolant temperature at the FA outlet, measured by the thermocouple and the average measured coolant temperature at the FA outlet for the given group, respectively, M_j – is the number of FA with thermocouples in group j.

The standard deviation characterizing the accuracy of coolant temperature measurement using the thermocouples in group j was determined by the formula

$$\sigma_j (T_{mes}^{i} - T_{av}^{j}) = (\sum_{i=1}^{M_j} (T_{mes}^{i} - T_{av}^{j})^2 / (M_j - 1))^{1/2} \qquad (1.2)$$

The deviation σ_j determined in this manner characterizes precisely the random error since in the calculation of the individual error by formula (1.1) its systematic part common for the given group of FAs disappears. Furthermore, it follows from formula (1.1, 1.2) that the mean group deviation from the T_{av}^{j} average for the "orbit", is equal to zero.

Using formula (1.2) the standard deviation for each group of symmetric FAs can be determined. For all the fuel assemblies or separated FAs groups to be jointly analyzed, it is necessary to know the character of distribution of individual measurement errors. In particular, it is desirable to be sure if the distribution of the whole set of errors is normal (or at least nearly normal) and also to know where the center of the density of individual error distribution is located.

The answer to the second question is clear as within each group of symmetrical fuel assemblies the average deviation (center) is equal to zero. The character of measurement error distribution was determined on the basis of Kolmogorov and/or Pearson criteria.

Since the number of operable thermocouples in different symmetry groups can differ essentially, the direct comparison of standard deviation σ_j is not informative. There are special criteria (e.g., Bartlett criterion), which permit to establish significantly or not the difference between dispersions σ^2_j and their corresponding standard σ_j at different volumes of samples. If the group dispersions σ^2_j, $j=1,2\ldots,N$ do not differ significantly, they belong to the same general sequence with the mean-weight dispersion

$$\sigma^2 = \frac{\sum_{j=1}^{N}(M_j - 1)\sigma_j^2}{\sum_{j=1}^{N}(M_j - 1)}. \qquad (1.3)$$

Here N is the number of fuel assemblies, the rest of notation has been defined above.

This dispersion corresponds to the mean-weight standard deviation σ characterizing the random error of the coolant temperature measurement at the fuel assembly outlet for the whole set of fuel assemblies of loading or for some separated FAs group.

1.3 PRINCIPLE OF MEASUREMENT DATA SCREENING

An important factor in performing statistical estimations is the absence of blunders in the measurements. Furthermore, the comparison of the measurement data with calculation results modeling the power unit operation should be also performed using the reliable initial data. Therefore the crude errors should be revealed and excluded from the consideration. In mathematics the problem of revealing errors of this type is called checking of observation uniformity.

When the mean value and the dispersion of the measured parameter for sampling are known (the true values are not known as a rule), the checking of uniformity is made on the basis of the τ-criterion. In our studies the measurement data not meeting the τ-criterion at the 5% significance level were rejected.

1.4 DEPENDENCE BETWEEN RANDOM VALUES

In performance of measurements in the operating power unit we deal with fuel assemblies of different types and powers. These fuel assemblies may posses their individual factors affecting the measurement error. In view of these reasons the dependence between random values may be “veiled”. The clarification of the character of dependences of this type is based on mathematical statistics methods.

There exists a stochastic relation between random values. The strength of stochastic relation is indicated by the coefficient of correlation. When the latter is nearly 1, the relation between the random values is the about to linear one. (This is an important aspect because the connection between the fuel assembly power and coolant heating is close to the linear one,

and an essential difference of the correlation coefficient from 1 will indicate deficiencies of the measurement system or any other problems).

The quantitative answer to the question on the dependence of the measured values of coolant temperature on the fuel assembly power can be obtained from the comparison of the mean values for the fuel assemblies of the same type, to which the same calculated power is ascribed. In mathematical statistics the dependence of the measured values is described by the equation of approximated regression. Since the regression equation is approximated, usually the type of its approximation is first chosen. As stated above, the relation between the fuel assembly power and coolant heating is close to the linear one. Therefore the most suitable approximation of ΔT_{ass} dependence on k_q will be linear. At an equal coolant temperature at the fuel assembly inlet the dependence between the coolant temperature at the fuel assembly outlet T_{ass}^{out} and the fuel assembly power is also close to the linear one.

As the equation of approximated regression are approximated with their statistic characteristics (dispersion and correlation coefficient), for them a confidence interval can be built, where the line of true regression (true dependence) lies with a probability of, for example, 95%.

1.5 RESULTS OF STATISTICAL ANALYSIS

It was established that for the fuel loadings considered the character of distribution of individual measurement errors is normal or close to normal. As the measurement error for all the set of fuel assemblies in the fuel loading the double mean-weight standard determined via standard deviations in the symmetrical groups of fuel assemblies was adopted. As follows from the Bartlett criterion, the group (sample) errors pertain to one general succession which determines the measurement error of the whole set of fuel assemblies constituting the particular fuel loadings.

Table 1.1 presents some statistical data characterizing the quality of temperature measurements by the fuel assembly thermocouples. The results are given after rejecting the measurement data by the τ-criterion with the level of confidence 5%. The number of rejected readings of thermocouples was 5-8%.

Table 1.1

Mean-weighting errors of the coolant temperature measurements of Kola NPP-3 and NPP-4 fuel loadings

Number of state	the 17th loading of unit 4		the 18th loading of unit 4		the 19th loading of unit 3		the 20th loading of unit 3	
	σ, °C	σ, % (*)	σ, °C	σ, %(*)	σ, °C	σ, %(*)	σ, °C	σ, %(*)
1 (BOC)	0.73	2.0	0.71	2.0	0.58	1.6	0.51	1.6
2	0.73	2.0	0.71	2.0	0.52	1.5	0.62	1.9
3	0.70	1.9	0.69	2.0	0.49	1.4	0.57	1.7
4	0.56	1.5	0.64	1.8	0.52	1.4	0.43	1.3
5	0.57	1.5	0.64	1.8	0.58	1.6	0.44	1.4
6 (EOC)	0.54	1.5	0.65	1.8	0.57	1.5	0.39	1.2

(*) $\sigma(\Delta T_{ass}/(T_{ass}^{out} - T_{ass}^{in}))$ – the mean-weight error relative to coolant heating in the fuel assembly.

Table 1.2 shows the correlation coefficients determining the degree of the linearity of approximated regressions (dependences between the random values) of coolant heating in the fuel assemblies and the relative power of FAs.

Table 1.2

Correlation coefficients of a coolant heatings and fuel assemblies power for the Kola NPP-3 and NPP-4

Number of state	the 17th loading of unit 4		the 18th loading of unit 4		the 19th loading of unit 3		the 20th loading of unit 3	
	FA without Gd	FA with Gd	FA without Gd	FA with Gd	FA without Gd	FA with Gd	FA without Gd	FA with Gd
1 (BOC)	0.998	0.985	0.997	0.990	0.995	0.964	0.997	0.971
2	0.997	0.981	0.997	0.990	0.995	0.968	0.996	0.970
3	0.998	0.983	0.997	0.990	0.995	0.978	0.997	0.970
4	0.998	0.976	0.997	0.987	0.996	0.977	0.997	0.964
5	0.998	0.977	0.997	0.987	0.996	0.971	0.997	0.960
6 (EOC)	0.998	0.977	0.997	0.986	0.996	0.971	0.997	0.961

As follows from Table 1.2 the approximation dependences of coolant temperature in the fuel assemblies are very close to the linear ones for all the types of fuel assemblies constituting the fuel loadings considered.

2. CHOICE OF FORMULA FOR CORRECTION CALCULATION

The data measured in the actual operating of the power unit known with some error. This affects the accuracy of determination of the correction accounting for the difference of the coolant temperature measured at the fuel assembly outlet from its average-mixed value. To reduce the effect of inaccuracies of the initial data on the correction value we have chosen such its type that, in our opinion, is less sensitive to the change in all the reactor parameters.

$$\delta T_{ass}^{i} / \Delta T_{ass}^{i} = (T_{TC}^{i} - T_{ass}^{i,av}) / (T_{TC}^{i} - T_{in}^{i}) \qquad (2.1)$$

Here T_{TC}^{i} is the readings of fuel assembly thermocouple, $T_{ass}^{i,av}$ is the average mixing value of coolant temperature at the outlet of fuel rod bundle, T_{in}^{i} is the coolant temperature at the fuel assembly inlet, ΔT_{ass}^{i} is the measured coolant heating in the fuel assembly.

Basing on the special calculations it was established that the influence of deviations of the reactor parameters from the nominal values (power, flow rate, pressure, and inlet coolant temperature) on the correction value calculated by formula (2.1) is very small.

Figs. 2.1-2.6 show the time dependences of (2.1) corrections for fuel assemblies of different types, constituting the fuel loadings considered. The notation in the figures corresponds to that used in formula (2.1).

Fig. 2.1. Dependence of corrections to the thermocouple readings for Gd-1 fuel assemblies of 1st year operation, fuel loading 17, power unit 4

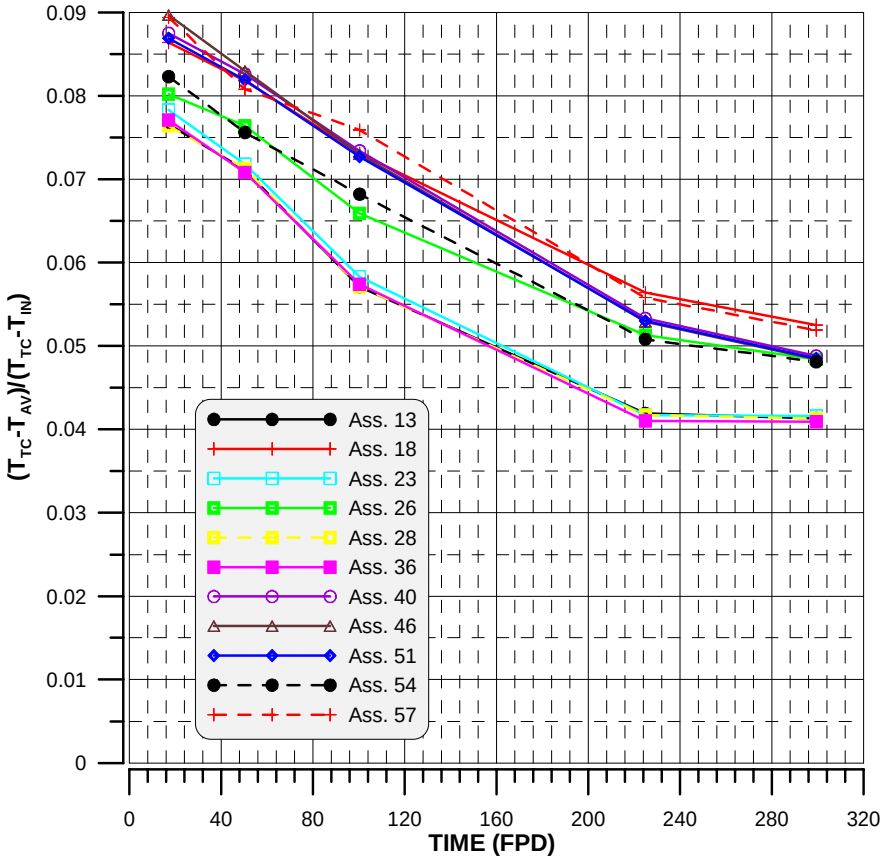

Fig.2.2. Dependence of corrections to the thermocouple readings for Gd-1 fuel assemblies of 2nd year operation, fuel loading 17, power unit 4.

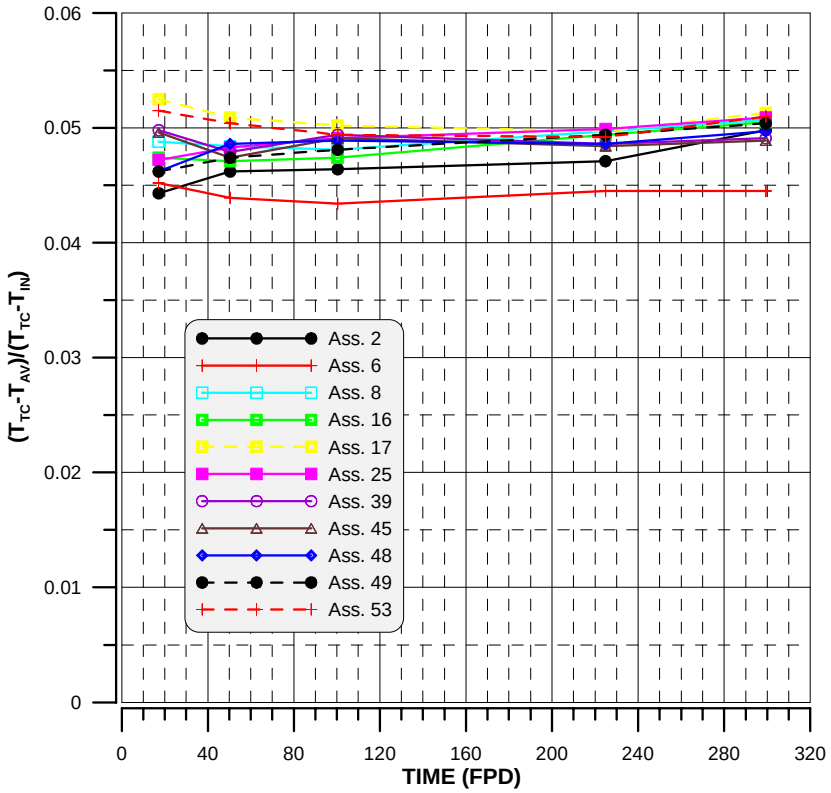

Fig.2.3. Dependence of corrections to the thermocouple readings for fuel assemblies with fuel without Gd of 3-5th year of operation, fuel loading 17, unit 4, cover size 145 mm.

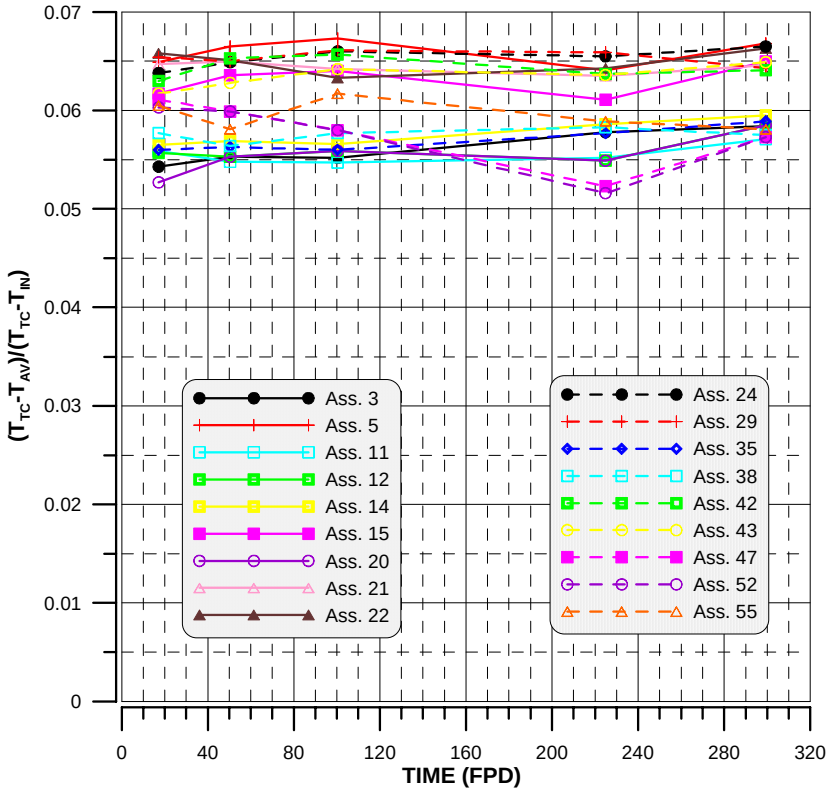

Fig.2.4. Dependence of corrections to the thermocouple readings for Gd-2 fuel assemblies of 1st year operation, fuel loading 19, power unit 3.

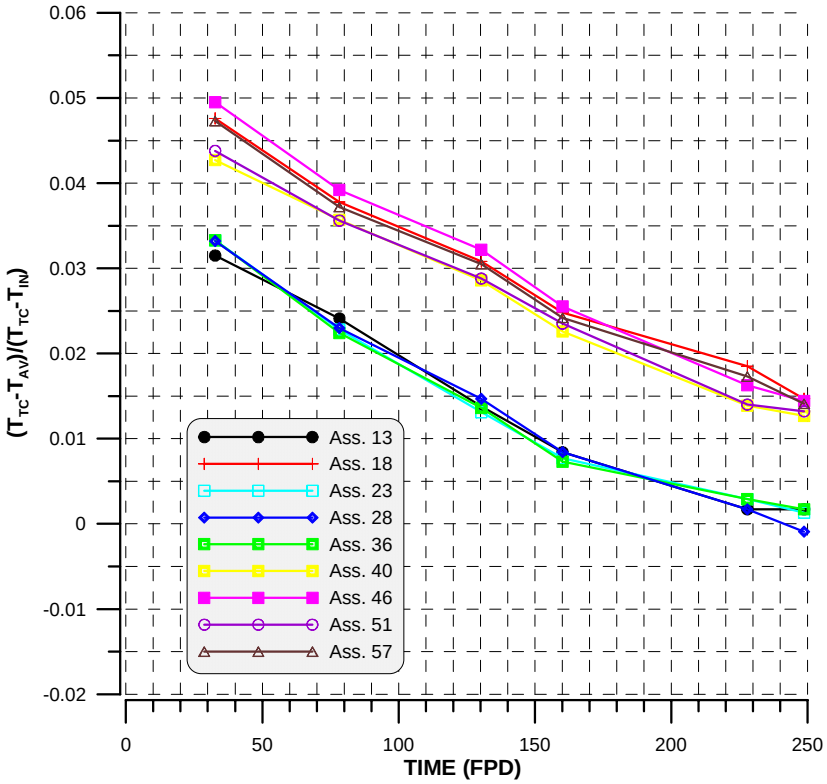

Fig.2.5. Dependence of corrections to the thermocouple readings for Gd-2-fuel assemblies of 2nd year operation, fuel loading 19, power unit 3.

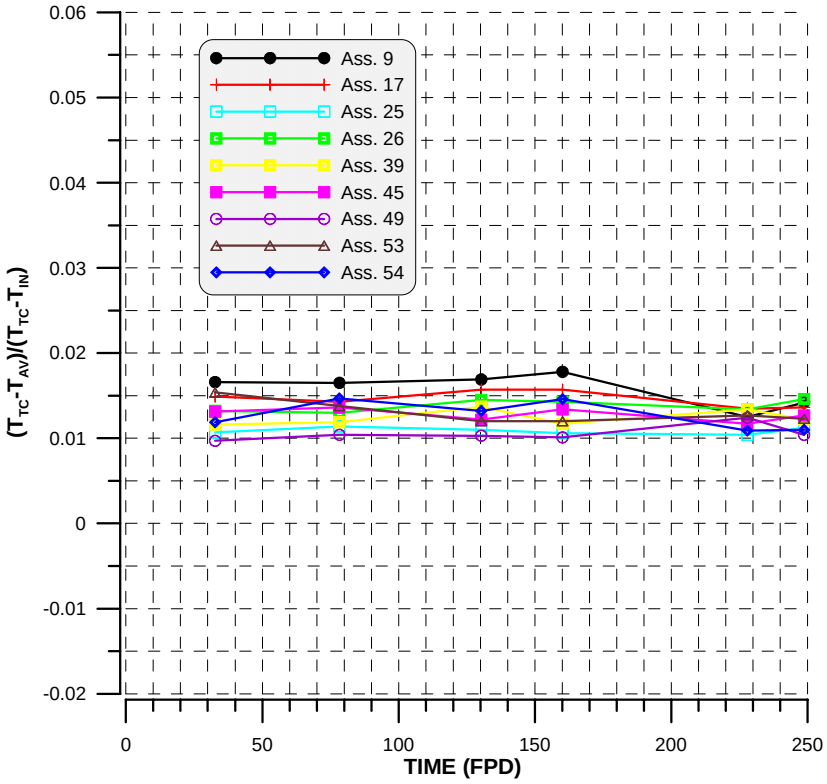

Fig. 2.6. Dependence of corrections to the thermocouple readings for fuel assemblies without Gd, 4-6th year operation, fuel loading, unit 3, cover size 143 mm.

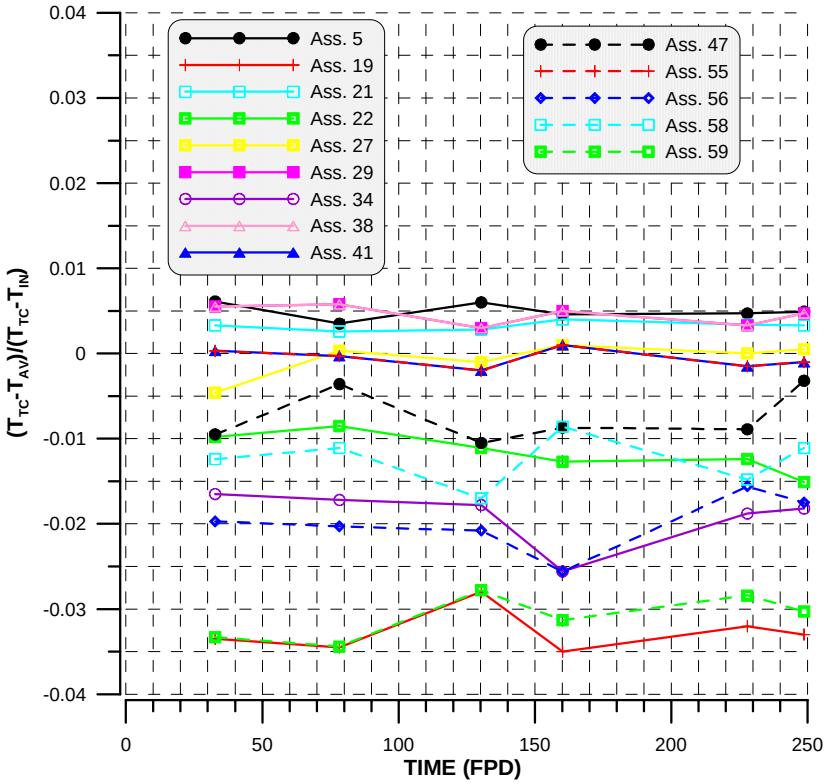

As follows from Figs. 2.1-2.6 for the fuel assemblies with Gd-1 and Gd-2 fuel the dependence of correction on time (burnup) is essential during the first year of operation. This is due to burnup of Gd_2O_3 absorber and power redistribution over the FA cross section. For the rest of fuel assemblies the value of the correction is more likely determined by the type of fuel assembly and, partially, on its location in the core. The main factor affecting the correction value is the pin-by-pin power distribution in the fuel assembly. Basing on the results of a series of experiments it was decided to approximate the correction by the linear function of the relative power of 36 central fuel rods (the approximation of the powers of 18 and 60 fuel rods was also were checked).

$$\delta T^i_{ass} / \Delta T^i_{ass} = F(q^i_{36}) = a + b q^i_{36}, \qquad (2.2)$$

where a and b are the approximation coefficients depending on the FA type, q^i_{36} is the relative power of 36 central fuel rods in the *i-th* fuel assembly.
In the calculations of FA power the thermocouple reading is corrected by the formula

$$T^{av}_{ass} = T^{i,mes}_{ass}(1 - \delta T^i_{mes} / \Delta T^{i,mes}_{ass}). \qquad (2.3)$$

Here $T^{i,mes}_{ass}$ is the thermocouple reading in the *i-th* fuel assembly,
$\Delta T^{i,mes}_{ass}$ is the measured coolant heating in the *i-th* fuel assembly.

It also follows from the dependences shown in Figs. 2.1-2.6 that the values of corrections accounting for incomplete coolant mixing in the distance from the fuel bundle to the thermocouple, varies within a wide range depending on the FA types. (From $\delta T^i_{ass} / \Delta T^i_{ass} \approx 9\%$ for fresh Gd-1 fuel assemblies to $\delta T^i_{ass} / \Delta T^i_{ass} \approx -3.5\%$ for spent fuel assemblies of first generation with the cover size 143 mm).

3. CORRECTION DEPENDENCES FOR FUEL ASSEMBLIES OF DIFFERENT TYPES

On the basis of the results of simulating neutron-physical and thermohydraulic calculations the dependences of corrections to the FA thermocouple readings as a function of the relative power of 36 central fuel rods for FA of different types were obtained.

For illustration some of these dependences are shown in Figs. 3.1-3.4. It follows from them, in particular, that formula (2.2) is quite universal and reasonably approximates the calculated corrections for fuel assemblies of different types and operation years. The difference of the correction obtained basing on the approximation formula of its calculated value does not generally exceed 0.5% of coolant heating in the fuel assembly.

Fig.3.1. Correction dependence for Gd-1 fuel assemblies of 1st-5th years of operation, loading 18, unit 4.

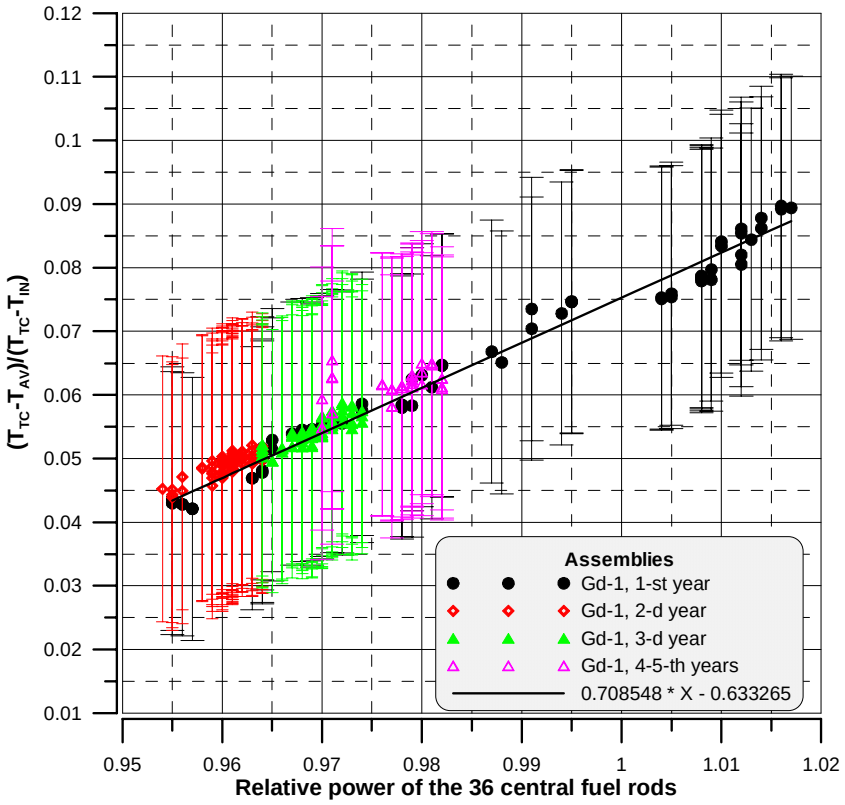

Fig.3.2. Correction dependence for Gd-2 fuel assemblies of 1st-3d years of operation, loading 20, unit 3.

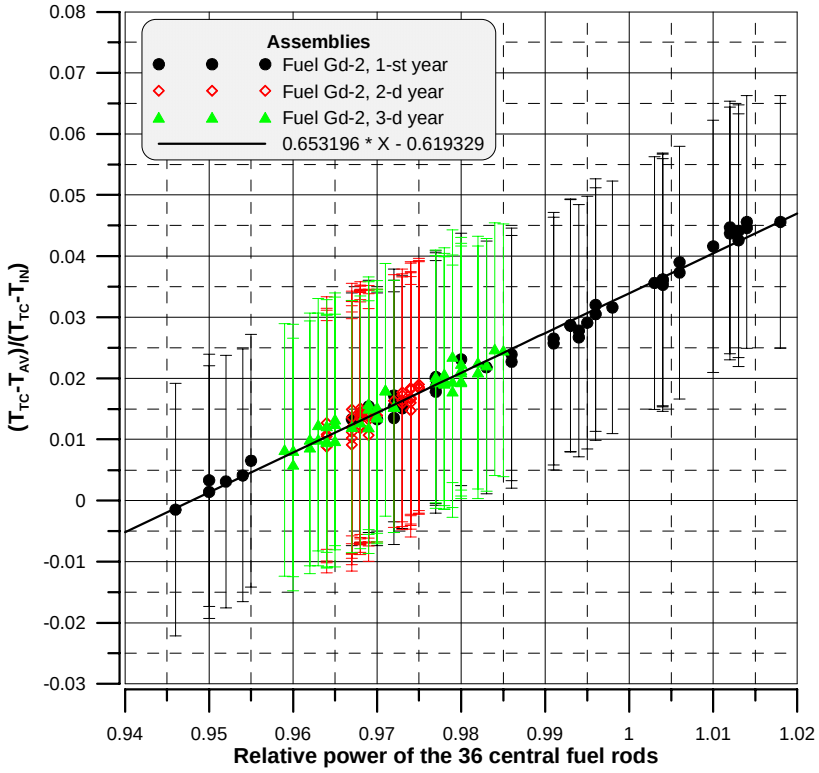

Fig.3.3. Correction dependence for 1st generation fuel assemblies without Gd of 3d-4th years of operation, loading 19, unit 3, cover size 145 cm.

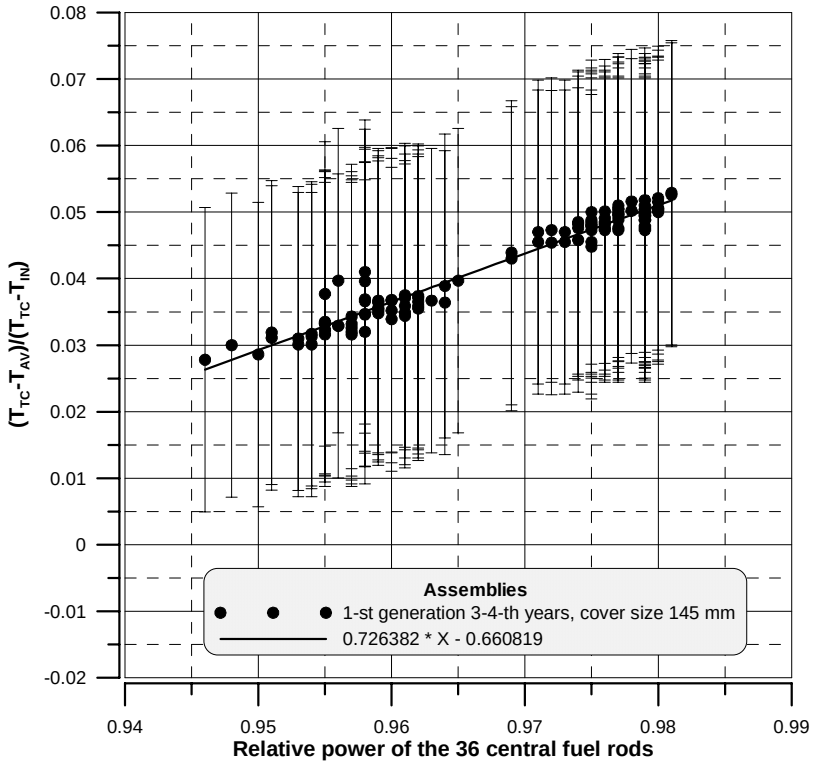

Fig.3.4. Correction dependence for 1st generation fuel assemblies without Gd of 4-6th years of operation, loading 19, unit 3, cover size 143 cm.

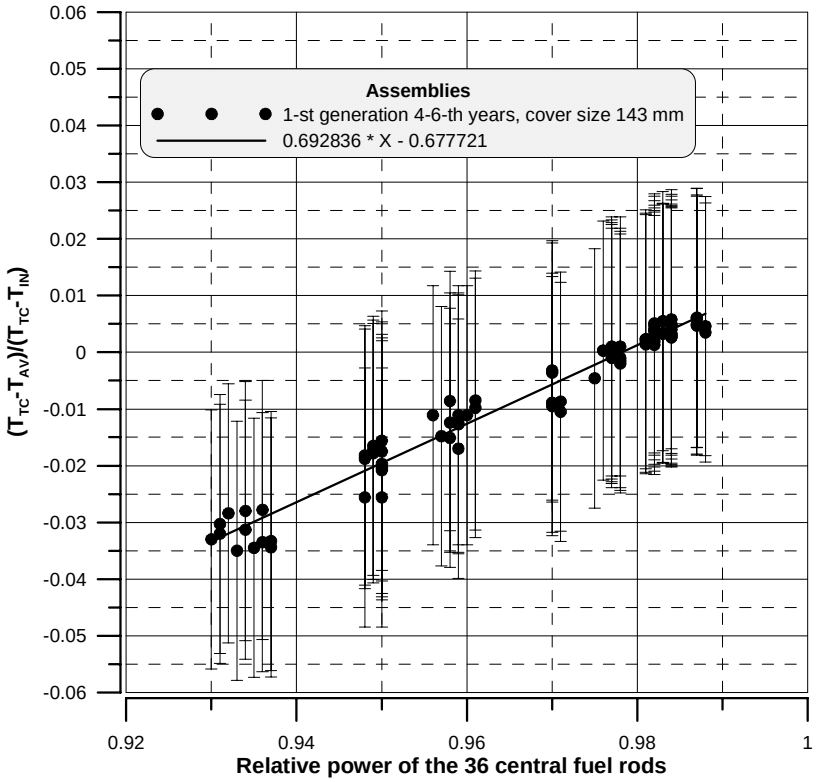

The correction dependences, presented in Figs.3.1-3.4 were obtained by the results of calculations simulating of NPP operation. They cannot be used for determination of FA powers by the thermal control data. For this purpose the approximation correction dependences should be obtained beforehand basing on a priori calculations, e.g. design ones. These calculations were also made for the considered fuel loadings of Kola NPP-3 and 4. The design calculations of neutron-physical characteristics were carried out at nominal core parameters which could differ essentially from the actual operation of the power units. Tables 3.1-3.4 list the main parameters for whose correction dependences were obtained. These dependences were used in the subsequent comparison of calculation and measured FA powers.

Table 3.1
Reactor parameters, 17th fuel loading of unit 4.

Design calculations					**Actual operation**				
T_{eff}, Day	**Power %**	**T_{inlet}, ^oC**	**H_{VI}, cm**	**Coolant flow rate, m^3/h**	**T_{eff}, Day**	**Power %**	**T_{inlet}, ^oC**	**H_{VI}, cm**	**Coolant flow rate, m^3/h**
20	**100**	**268**	**184.5**	**39200**	**17.2**	**100**	**266.5**	**215**	**39200**
60	**100**	**268**	**184.5**	**39200**	**50.4**	**99.6**	**266.6**	**184**	**39200**
100	**100**	**268**	**184.5**	**39200**	**100.4**	**100**	**266.6**	**181**	**39200**
220	**100**	**268**	**184.5**	**39200**	**224.8**	**99.7**	**267.2**	**223**	**39200**
281	**100**	**268**	**244**	**39200**	**299.3**	**98.7**	**266.5**	**250**	**39200**

Table 3.2
Reactor parameters, 18th fuel loading of unit 4.

Design calculations					Actual operation				
T_{eff}, Day	Power %	T_{inlet}, °C	H_{VI}, cm	Coolant flow rate, m^3/h	T_{eff}, Day	Power %	T_{inlet}, °C	H_{VI}, cm	Coolant flow rate, m^3/h
20	100	268	202.4	39200	22	98.0	264.4	192	39200
40	100	268	202.4	39200	35.3	97.0	263.4	193	39200
100	100	268	202.4	39200	104.6	95.0	263.6	181	39200
160	100	268	202.4	39200	154	98.0	263.6	187	39200
200	100	268	202.4	39200	205.3	100	265.6	202	39200
220	100	268	202.4	39200	214.8	95.1	265.7	195	39200

Table 3.3
Reactor parameters, 19th fuel loading of unit 3.

Design calculations					Actual operation				
T_{eff}, Day	Power %	T_{inlet}, °C	H_{VI}, cm	Coolant flow rate, m^3/h	T_{eff}, Day	Power %	T_{inlet}, °C	H_{VI}, cm	Coolant flow rate, m^3/h
40	100	268	202.4	40013	32.7	100	264.4	175	40850
80	100	268	202.4	40013	78.3	99.3	263.4	192	40850
140	100	268	202.4	40013	130.3	98.5	263.6	198	40850
160	100	268	202.4	40013	160.1	99.9	263.6	190	40850
220	100	268	202.4	40013	227.9	100	265.6	199	40850
240	100	268	202.4	40013	248.7	99.4	265.7	215	40850

Table 3.4
Reactor parameters, 20th fuel loading of unit 3.

Design calculations					Actual operation				
T_{eff}, Day	Power %	T_{inlet}, °C	H_{VI}, cm	Coolant flow rate, m^3/h	T_{eff}, Day	Power %	T_{inlet}, °C	H_{VI}, cm	Coolant flow rate, m^3/h
40	100	268	202.4	40013	44.3	96.2	264.4	195	40850
80	100	268	202.4	40013	77.7	95.6	264.9	222	40850
120	100	268	202.4	40013	121.6	97.0	264.5	207	40850
200	100	268	202.4	40013	198.4	95.3	264.5	222	40850
260	100	268	202.4	40013	254.3	95.1	267.0	222	40850

As follows from Table 3.1-3.4 the difference in the core parameters at which a priori and a posteriori calculations on the determination of correction dependences were carried out could be essential. In particular, the difference in the inlet coolant temperature was up to 4°C and more, in the coolant flow rate – up to 2%, in the reactor power up to 5% nominal, with the control group position up to 40 cm.

The maximum difference in the values of corrections obtained in two ways, was ~ 0.8% of coolant heating in the fuel assembly for low-power assemblies (k_q~0.3÷0.4). For all the types of the high-power fuel assemblies (k_q~1.2 ÷ 1.45) the difference in the correction values obtained on the basis of a priori and a posteriori calculations does not exceed 0.2% of coolant heating in the fuel assembly.

4. COMPARISON OF CALCULATION RESULTS WITH MEASUREMENT DATA

To be sure about the correctness of the approach to accounting for incomplete coolant mixing, proposed in this paper, calculations on the comparison of measured and calculated assembly-by-assembly power distributions were carried out.

In the first case the measurement results were used by the traditional method without introducing any corrections for the difference between the measured and average mixing coolant temperatures. In the three other cases the corrections obtained using different methods were introduced:

1. corrections were determined by the results of direct calculations of all the fuel assemblies in the fuel loadings considered, by the modernized version of SC-1 code (calculated corrections);
2. corrections obtained in number 1 way, were approximated by the dependences similar to (2.2), and these dependences were used in the determination of relative FA powers by the thermocouple readings (a posteriori correction dependences);
3. on the basis of the results of design calculations of the neutron-physical characteristics and subsequent SC-1 code calculations the approximation correction dependences were obtained, which also were used in the determination of relative FA powers (a priori correction dependences).

The “measured” values of relative FA powers, obtained by these methods were compared with k_q values obtained in the calculations of neutron-physical characteristics, made in the regime of simulation of the Kola NPP-3 and 4 operations in accordance with the loading schedules.

In principle, a good agreement of the calculation results with the measurement data (with account for the corrections) is not guarantee of correctness of corresponding corrections, in itself. In some fuel assemblies this agreement may even deteriorate since the measurements are made with the finite accuracy, and there exists a certain dispersion of the values of quantities measured. Nevertheless, for the whole set of fuel assemblies (for representative statistical sample) better coincidence of calculation results with the measurement data should be observed in the proper introduction of corrections.

The three above methods for introduction of correction dependences should have demonstrated:

1. advisability of introducing corrections for incomplete coolant mixing in the fuel assembly;
2. possibility of replacing the calculation corrections by approximation dependences;
3. possibility of obtaining these dependences at the design stage of fuel assemblies loadings with their subsequent use in the ICIS software.

In the comparison of the calculated and “measured” values of relative FA powers the variant for which during the fuel cycle the deviation of calculation k_q value from the “measured” one, maximum in its absolute value, was smaller.

If the results obtained are summed, then, basing on the four fuel loadings of Kola NPP-3 and NPP-4, the main conclusions can be formulated as follows:

- in the calculation of the relative power of fuel assemblies, with account for corrections to incomplete coolant mixing in the FA head in the form of approximation dependence (2.2), the agreement between the calculation and measurement results was improved in 158 cases from the total number of 208 fuel assemblies (symmetry sector 60^o, four fuel loadings, 52 fuel assemblies in each symmetry sector);
- in the 21 fuel assembly the result did not practically change;
- in the 29 cases the agreement of the calculation results with the measurement data deteriorated after introduction of correction for incomplete mixing of the coolant in its moving to the thermocouple (these are mainly low-power fuel assemblies).

If two variants, where the result was either improved or not deteriorated, are combined, then the effect of introducing such a correction will amount to about 86%.

Along with the individual values of differences between the calculation and measurement results (for illustration these differences are given in Figs. 4.3-4.55 of Appendix) some generalized statistical characteristics were calculated. In particular, samples of fuel assemblies with the relative power higher or lower than 1 were considered. For these FA the root-mean-square deviations of the calculation relative powers from the "measured" ones, as well as mean sample deviations were calculated.

As the calculation and "measured" values of relative FA powers are determined in the same normalization the mean deviation for the whole set of fuel assemblies is equal to zero. The calculation results are listed in Tables 4.1-4.4.

Table 4.1

Effective statistical characteristics, 17^{th} fuel loading of unit 4

T_{eff}, day	Without correction			With correction		
	$\sigma(k_q^{cal}-k_q^{mes})$ $(k_q>1)$	$\sigma(k_q^{cal}-k_q^{mes})$ $(k_q<1)$	$(k_q^{cal}-k_q^{mes})_{av}$ $(k_q>1)$	$\sigma(k_q^{cal}-k_q^{mes})$ $(k_q>1)$	$\sigma(k_q^{cal}-k_q^{mes})$ $(k_q<1)$	$(k_q^{cal}-k_q^{mes})_{av}$ $(k_q>1)$
17.2	**0.0312**	**0.0246**	**0.0079**	**0.0239**	**0.0155**	**0.0018**
50.4	**0.0332**	**0.0214**	**0.0104**	**0.0249**	**0.0142**	**0.0022**
100.4	**0.0331**	**0.0209**	**0.0068**	**0.0251**	**0.0138**	**-0.0012**
224.8	**0.0325**	**0.0230**	**0.0079**	**0.0257**	**0.0132**	**0.0016**
299.3	**0.0321**	**0.0222**	**0.0052**	**0.0242**	**0.0142**	**0.0010**

Table 4.2
Effective statistical characteristics, 18th fuel loading of unit 4

T_{eff}, day	Without correction			With correction		
	$\sigma(k_q^{cal} - k_q^{mes})$ $(k_q > 1)$	$\sigma(k_q^{cal} - k_q^{mes})$ $(k_q < 1)$	$(k_q^{cal} - k_q^{mes})_{av}$ $(k_q > 1)$	$\sigma(k_q^{cal} - k_q^{mes})$ $(k_q > 1)$	$\sigma(k_q^{cal} - k_q^{mes})$ $(k_q < 1)$	$(k_q^{cal} - k_q^{mes})_{av}$ $(k_q > 1)$
22.0	**0.0279**	**0.0196**	**0.0062**	**0.0196**	**0.0168**	**-0.0016**
35.3	**0.0279**	**0.0197**	**0.0062**	**0.0196**	**0.0168**	**-0.0014**
104.6	**0.0279**	**0.0191**	**0.0043**	**0.0190**	**0.0180**	**-0.0016**
154.0	**0.0271**	**0.0200**	**0.0110**	**0.0201**	**0.0164**	**0.0060**
205.3	**0.0274**	**0.0191**	**0.0114**	**0.0208**	**0.0150**	**0.0065**
214.8	**0.0275**	**0.0192**	**0.0110**	**0.0209**	**0.0150**	**0.0061**

Table 4.3
Effective statistical characteristics, 19th fuel loading of unit 3

T_{eff}, day	Without correction			With correction		
	$\sigma(k_q^{cal} - k_q^{mes})$ $(k_q > 1)$	$\sigma(k_q^{cal} - k_q^{mes})$ $(k_q < 1)$	$(k_q^{cal} - k_q^{mes})_{av}$ $(k_q > 1)$	$\sigma(k_q^{cal} - k_q^{mes})$ $(k_q > 1)$	$\sigma(k_q^{cal} - k_q^{mes})$ $(k_q < 1)$	$(k_q^{cal} - k_q^{mes})_{av}$ $(k_q > 1)$
32.3	**0.0456**	**0.0292**	**0.0384**	**0.0317**	**0.0268**	**0.0149**
78.3	**0.0445**	**0.0300**	**0.0375**	**0.0310**	**0.0272**	**0.0132**
130.3	**0.0442**	**0.0316**	**0.0365**	**0.0319**	**0.0248**	**0.0152**
160.1	**0.0420**	**0.0318**	**0.0364**	**0.0319**	**0.0250**	**0.0160**
227.9	**0.0428**	**0.0310**	**0.0369**	**0.0327**	**0.0244**	**0.0174**
248.7	**0.0427**	**0.0310**	**0.0368**	**0.0327**	**0.0243**	**0.0170**

Table 4.4
Effective statistical characteristics, 20th fuel loading of unit 3

T_{eff}, day	Without correction			With correction		
	$\sigma(k_q^{cal} - k_q^{mes})$ $(k_q > 1)$	$\sigma(k_q^{cal} - k_q^{mes})$ $(k_q < 1)$	$(k_q^{cal} - k_q^{mes})_{av}$ $(k_q > 1)$	$\sigma(k_q^{cal} - k_q^{mes})$ $(k_q > 1)$	$\sigma(k_q^{cal} - k_q^{mes})$ $(k_q < 1)$	$(k_q^{cal} - k_q^{mes})_{av}$ $(k_q > 1)$
32.3	**0.0351**	**0.0258**	**0.0051**	**0.0258**	**0.0205**	**0.0006**
78.3	**0.0351**	**0.0259**	**0.0067**	**0.0258**	**0.0206**	**0.0026**
130.3	**0.0348**	**0.0261**	**0.0068**	**0.0257**	**0.0209**	**0.0028**
160.1	**0.0332**	**0.0269**	**0.0054**	**0.0245**	**0.0225**	**0.0019**
248.7	**0.0333**	**0.0262**	**0.0088**	**0.0260**	**0.0204**	**0.0036**

As follows from the data shown in Tables 4.1-4.4 the taking into account of corrections for incomplete coolant mixing decreases the root-mean square deviation for fuel assemblies of one and the other groups in all the fuel loadings considered. This means that the spread of values $(k_q^{i,cal} - k_q^{i,mes})$ decreases. With introducing the correction the absolute value of average deviation of the calculation values from the "measured" ones also decreases. The decrease in the average deviation of the calculation values of relative FA powers from the "measured" ones indicates the decrease in precisely the systematic constituent of the error.

As far as the high power fuel assemblies are concerned, which are of the primary interest to us, for them the introduction of correction dependences taking into account the incomplete coolant mixing in the distance from the fuel pin bundle to the fuel assembly thermocouple also allows, the systematic constituent of measurement error to be reduced. This follows from the comparison of dependences shown in Figs.4.1, 4.2.

Fig. 4.1. Deviations of calculation values of fuel assembly powers from the measured ones, unit 3, fuel loading 19, the sample of fuel assemblies with relative power higher than 1.2, without correction for the incomplete coolant mixing

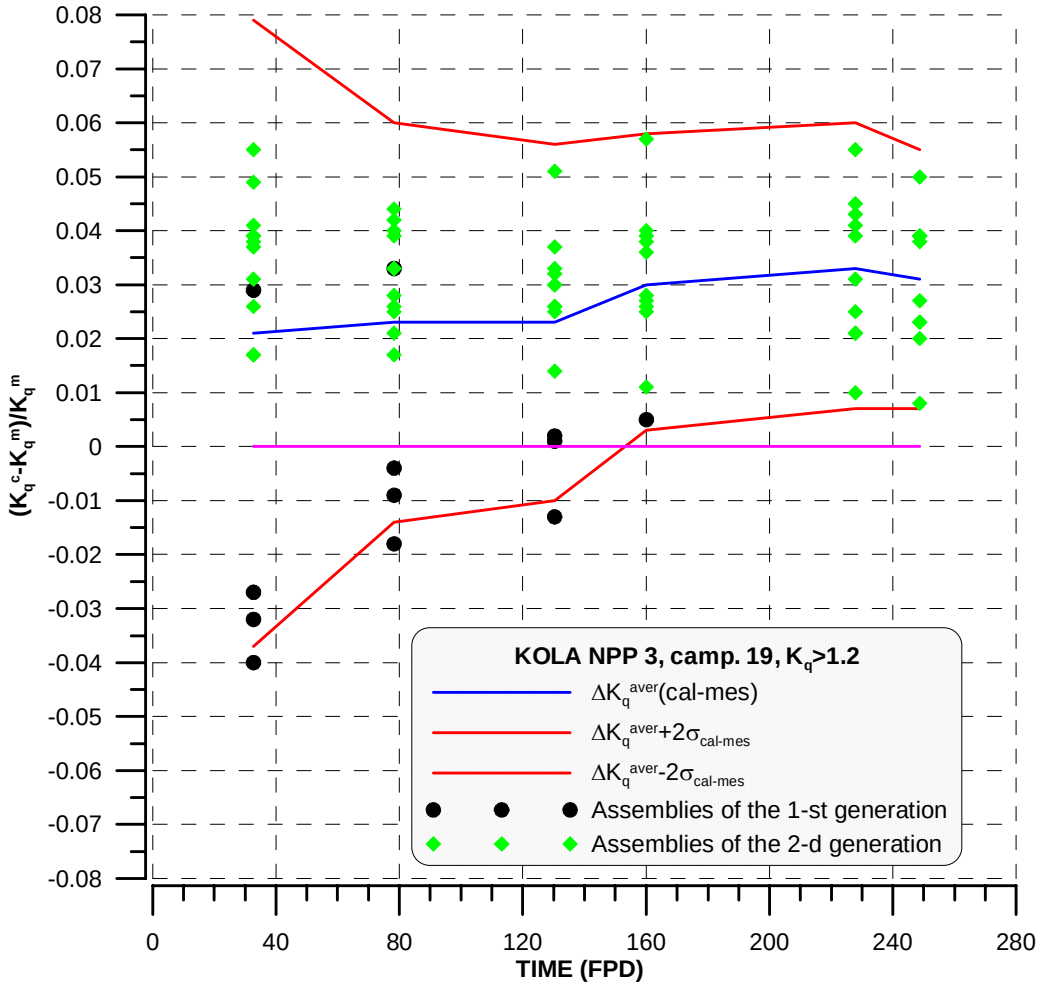

Fig.4.2. Deviations of calculation values of fuel assembly powers from the measured ones, unit 3, fuel loading 19, the sample of fuel assemblies with relative power higher than 1.2, with the correction for the incomplete coolant mixing.

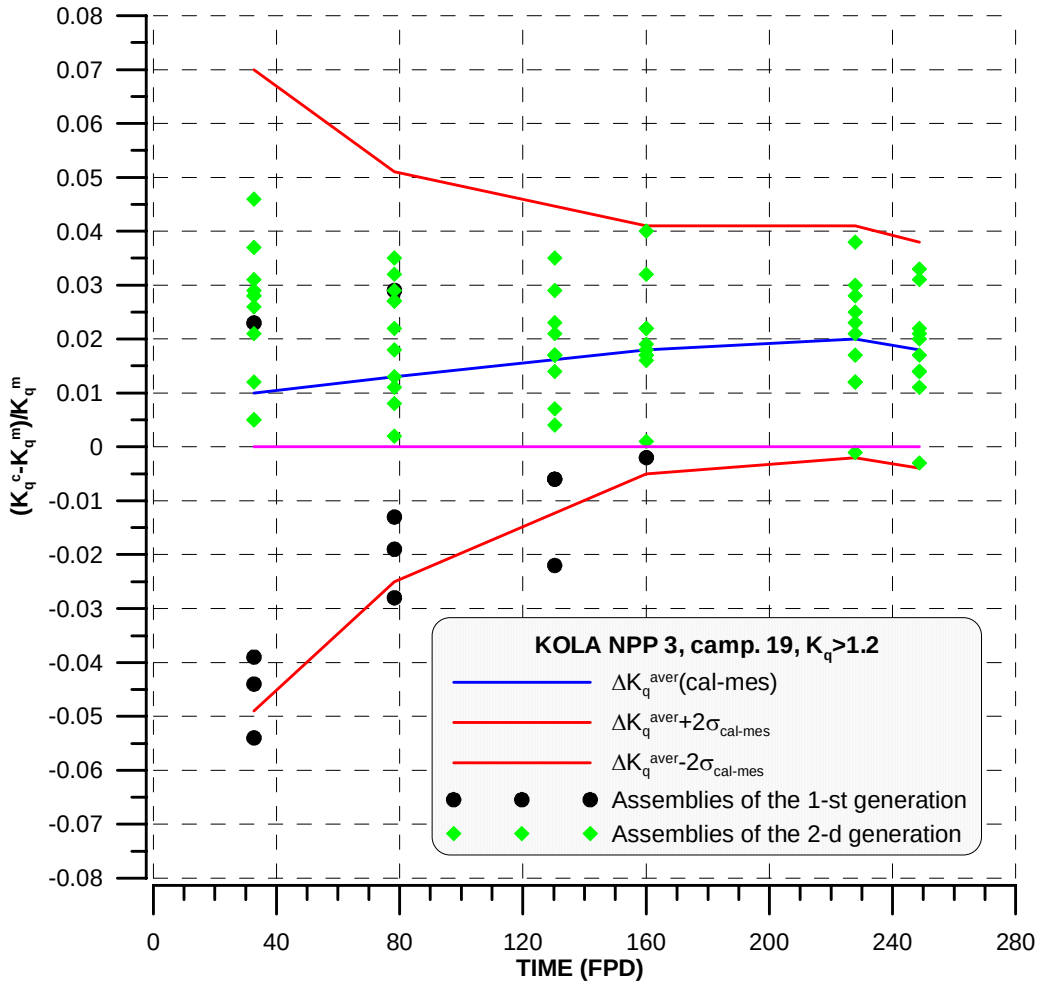

5. ASSESSMENT OF CORE BYPASS COOLANT FLOWS ACCORDING TO THE THERMAL CONTROL DATA

For the 19th and 20th fuel loadings of unit 3 the calculation assessment of core bypass flows was made. The assessment was based on the reactor measurement data and calculation determination of corrections accounting for the difference of fuel assembly thermocouple readings from the average mixing value of coolant temperature at the outlet of the fuel bundle.

The calculation of core bypass flows was carried out for different times of fuel cycle by the formula

$$Bypass = 1 - (\Delta I_{core} - \Delta I_R) / \Delta I_{core}. \quad (5.1)$$

Here ΔI_{core} is the average coolant heating in the core, determined by readings of fuel assembly thermocouples, ΔI_R is the coolant heating in the reactor, determined by readings of the loop thermocouples. The average coolant heating in the core ΔI_{core} was determined by three methods:

1. readings of fuel assembly thermocouples were used without any corrections;
2. readings of fuel assembly thermocouples were used taking into account corrections for radiation heating-up;
3. readings of fuel assembly thermocouples were used taking into account corrections for radiation heating-up and correction dependences accounting for the incomplete coolant mixing in the fuel assembly head.

In accordance with this the following results were obtained for 19th and 20th fuel loadings of Kola NPP-3:

1. without considering corrections the core bypass flows were 9.83-10.56 %;
2. taking into account radiation heating-up of thermocouples the bypass flows were 7.61-8.39 %;
3. taking into account radiation heating-up of thermocouples and correction dependences accounting for the incomplete coolant mixing in the fuel assembly head, the core bypass flows were 5.26-5.69 %.

Thus it may be concluded that the value of core bypass coolant flows is determined to a large extent depending on how readings of fuel assembly thermocouples are treated when the core bypass coolant flows are determined by the data of thermal control. It should be noted that the coolant passing between the fuel assemblies is also partially heated thus enabling the fuel pin cooling. As shown by the calculation results the coolant heating in the inter-assembly space is about 15-20 % of coolant heating in the adjacent fuel assemblies.

CONCLUSION

In the paper an approach to solving the problem of treating readings of the fuel assembly thermocouples which are used for the determination of relative fuel assembly powers, is briefly presented. Basing on the experimental data and calculation results it is pointed out that, in principle, the coolant temperature measured by the fuel assembly thermocouple may differ from the average mixing coolant temperature at the outlet of the fuel bundle, which characterizes the fuel assembly power. The degree of the difference depends on many factors determining the coolant temperature profile at the outlet coolant and the character of its mixing in the fuel assembly head. It follows from the calculation analysis, in particular, that in the fuel loadings for fuel assemblies of different types, considered in this work, the difference can be from $-(0.5 \div 1)\ ^{o}C$ to $1.5 \div 3\ ^{o}C$.

A method for obtaining correction dependences is briefly described. On the basis of experimental and calculation studies a type of corrections taking into account the incomplete coolant mixing in the fuel assembly was proposed. These corrections were conditionally called the calculation ones.

The use of approximation dependences instead of the calculation corrections showed that these corrections can be approximated by the linear function of the relative power of 36 central fuel rods. The approximation of correction dependences as a whole gives a close result as compared with that obtained in introducing the calculation corrections.

By the results of design calculations of neutron-physical characteristics, the a priori correction dependences were determined, which subsequently were also used in the comparison of the calculation and “measured” assembly-by-assembly power distributions fields.

The results obtained from the comparison of the calculation and “measured” relative fuel assembly powers indicate that the correction dependence obtained a priori by the results of the

design calculations can be used in the software of ICIS of the VVER-440 reactors for accounting for the incomplete coolant mixing in the fuel assemblies when determining their power by thermal control data.

The correction accounting for the incomplete coolant mixing in the fuel assembly is then determined by the formula

$$(\delta T^i_{ass} / \Delta T^i_{ass})_{mes} = a_{design} + b_{design} q^{design}_{i,36}$$

where the coefficients a_{design}, and b_{design} (depending on the type of fuel assembly), as well as the array of $q^{design}_{i,36}$ values should be obtained by the results of a priori design calculations and entered to the ICIS data base.

The assessment of core bypass coolant flow was carried out. For the19th and 20th fuel loadings of the Kola NPP-3 the following results were obtained:

1. without accounting for the correction the core bypass flows were 9.83 – 10.56 %;
2. with accounting for the radiation heating-up of the thermocouples the core bypass flows were 7.61 – 8.39 %;
3. with accounting for the radiation heating-up of the thermocouples and correction dependences taking into account the incomplete coolant mixing in the fuel assembly head the core bypass flows were 5.26 – 5.69 %.

All the results obtained are precisely characteristic of the units of Kola NPP. For other NPPs having their own fuel loadings, softwares and measuring instrumentation the results may quantitatively differ from those presented in this paper.

Actually the paper proposes a certain general approach to solving the problem of treating readings of fuel assembly thermocouples in the determination of fuel assembly powers by the data of thermocontrol. The interested parties may use this approach, fully or partially, taking into account the features characteristic of appropriate power units and NPPs.

In the paper the problem of introducing the correction dependences with the reactor operating at power essentially differing from the nominal power, was not reflected. In principle, the method for correcting the a priori correction dependences for their use at partial power levels was also developed. It requires performance of additional physical calculations simulating the reactor operation and entering additional data arrays to the ICIS variable data base. At the same time it should be noted that operation at low power does not require, in principle, an accurate determination of powers of the fuel assemblies and coolant heating in them.

Also the problem of introducing the correction dependences in reactor operation with incomplete number of loops was not considered. This question can be considered as one of possible directions for further investigation of the problem of accounting for the incomplete coolant mixing in the fuel assembly heads.

Finally, it should be said about the plans of loading of noncover three generation fuel assemblies having higher multiplying properties to the cores of Kola NPP units. The arrangement of these fuel assemblies in the core will require some additional investigations of the problem considered in this paper. This is due to both the absence of fuel assembly cover and to increasing the fuel lattice pitch up to 12.6 mm.

In conclusion it can be stated the following: at present, in principle, in the determination of relative fuel assembly powers, admissible coolant heating-ups in the fuel assemblies during the reactor operation the direct measurements of outlet coolant temperature can be used without introducing corrections. However the use of correction dependences would allow the systematical constituent of measurement error arising due to the incomplete coolant mixing in

the fuel assembly head to be reduced, the admissible coolant heating-up in the fuel assemblies and core bypass flows to be assessed more accurately. In addition, in this case the verification of neutron-physical codes by the reactor measurement data can be made more with higher accuracy.

REFERENCES

1. P. Kodl. Coolant Flow Calculation in VVER Fuel Assembly Outlet Part Using PHOENICS CFD Code. Hungary, 2005.
2. V. Petenyi, K. Klucarova, J. Remis. Fuel Assembly Outlet Temperature Profile Influence on Core Bypass Flow Power Distribution Determination in VVER-440 Reactors. VUJE Trnava, Germany, 2003.
3. G. Legardy, A. Aszordi. Detailed CFD Analysis of Coolant Mixing in VVER-440 Fuel Assembly Heads Performed with the Code CFX-5.5. Hungary, Germany, 2003.
4. T. Toppila, V. Lestinen, P. Siltanen. CFD-Simulation of Cooling Mixing Inside the Fuel Assembly Top Nozzle and Core Exit Channel of VVER-440 Reactor. Finland, 2004.
5. J. Kuusisto, M. Antila, P. Siltanen. Modelling of the Coolant Temperature Profile Efection Assembly Outlet Temperature Measurements in VVER-440 Reactors. Finland, 2004.
6. L. Kobzar, D. Oleksiuk. First Series of Experiments on Simulation of Coolant Mixing in Fuel Assembly Head and Core Exit Channel of VVER-440 Reactor. Annual meeting of WG G of AER, 2006.
7. The PHOENICS Reference Manual. CHAM TR/200 (PIL)
8. Testimonial of SC-1 code. Pasport №123. Moscow, 2000.

APPENDIX

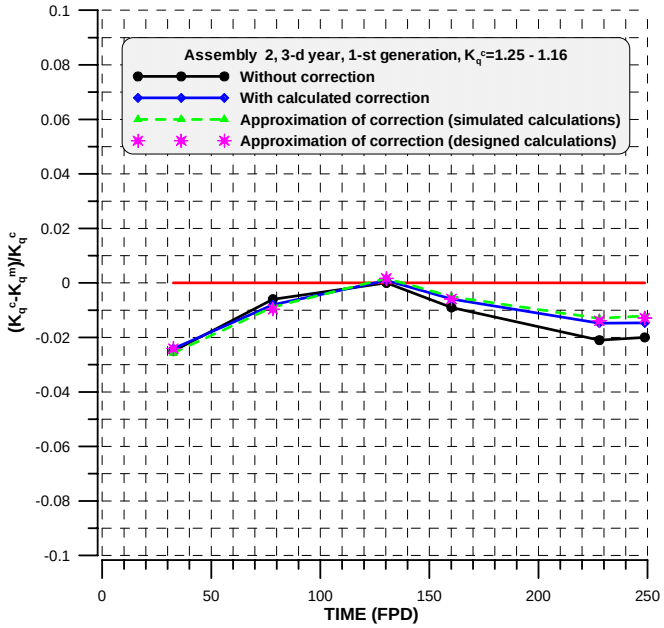

Fig. 4.3. Difference between calculated and measured relative assembly power during 20-th campaign. Assembly of the 1-st generation without Gd. Kola NPP Unit 3

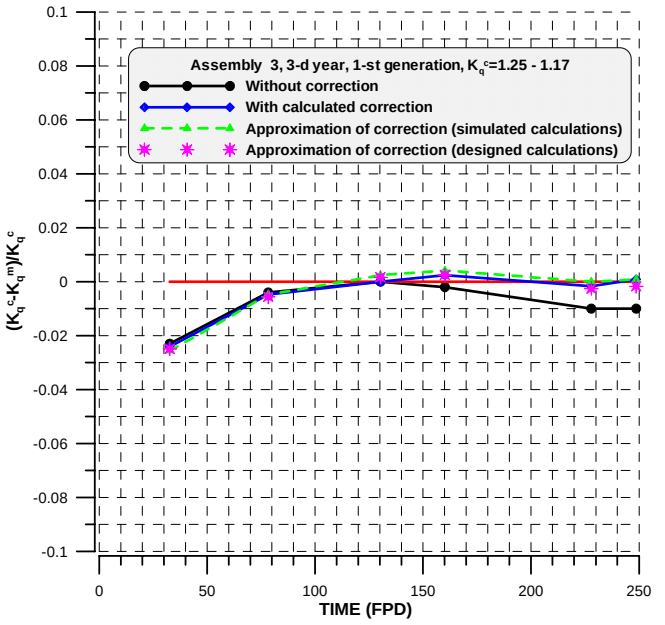

Fig. 4.4. Difference between calculated and measured relative assembly power during 20-th campaign. Assembly of the 1-st generation without Gd. Kola NPP Unit 3

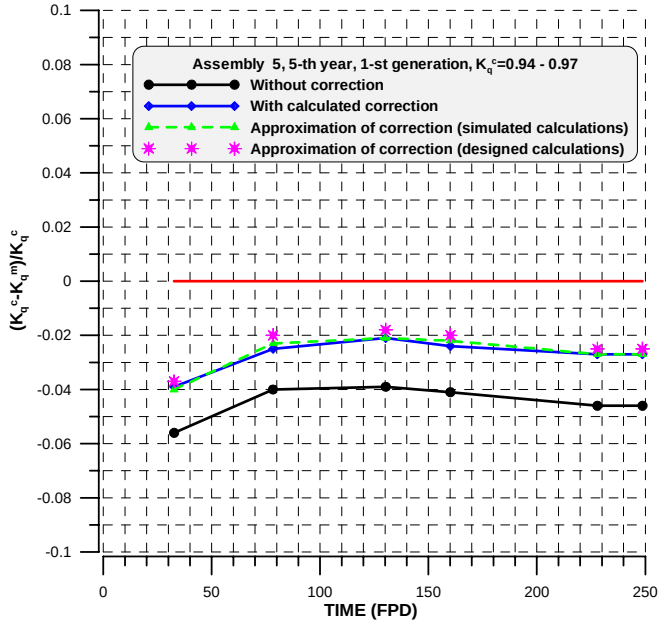

Fig. 4.5. Difference between calculated and measured relative assembly power during 20-th campaign. Assembly of the 1-st generation without Gd. Kola NPP Unit 3

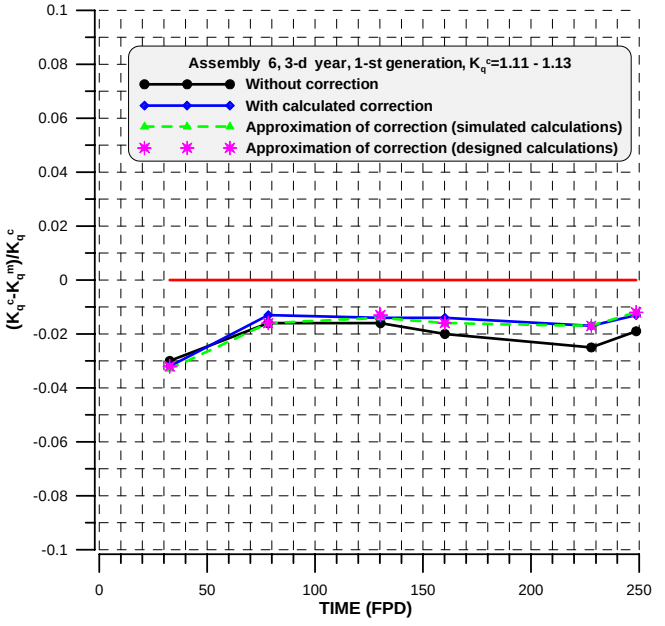

Fig. 4.6. Difference between calculated and measured relative assembly power during 20-th campaign. Assembly of the 1-st generation without Gd. Kola NPP Unit 3

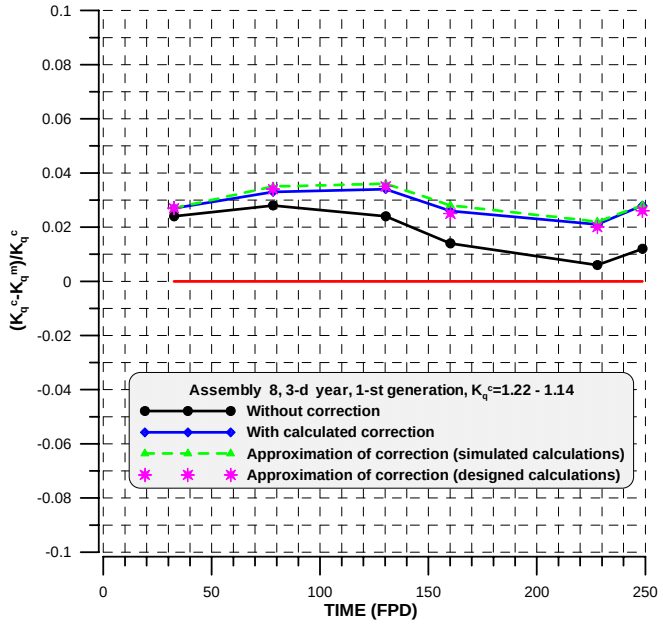

Fig. 4.7. Difference between calculated and measured relative assembly power during 20-th campaign. Assembly of the 1-st generation without Gd. Kola NPP Unit 3

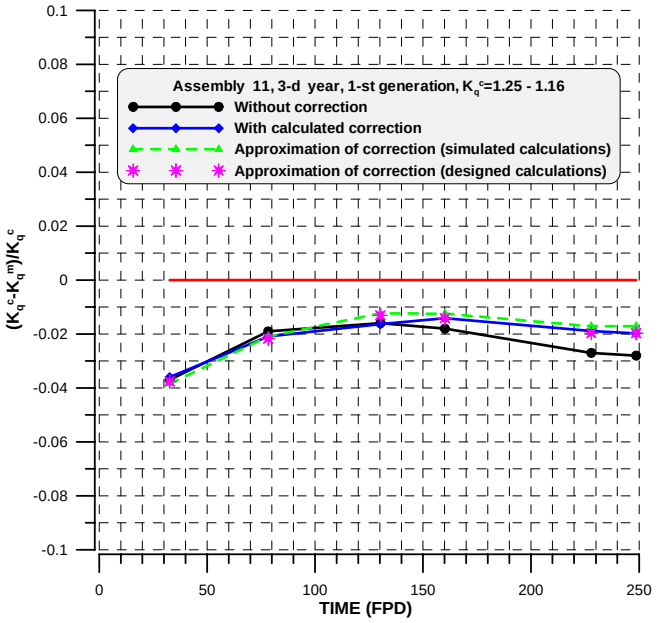

Fig. 4.8. Difference between calculated and measured relative assembly power during 20-th campaign. Assembly of the 1-st generation without Gd. Kola NPP Unit 3

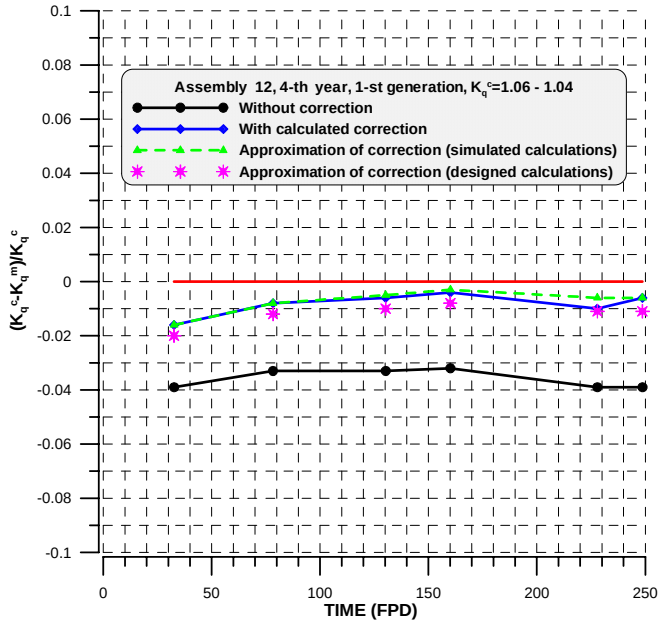

Fig. 4.9. Difference between calculated and measured relative assembly power during 20-th campaign. Assembly of the 1-st generation without Gd. Kola NPP Unit 3

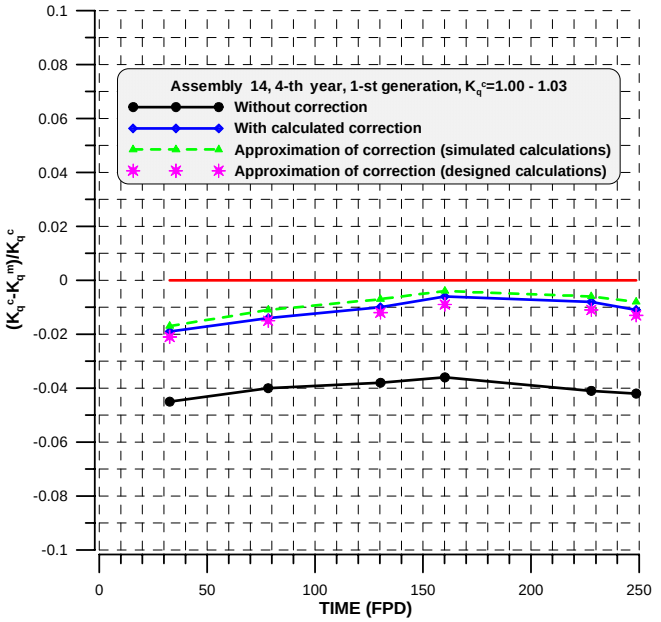

Fig. 4.10. Difference between calculated and measured relative assembly power during 20-th campaign. Assembly of the 1-st generation without Gd. Kola NPP Unit 3

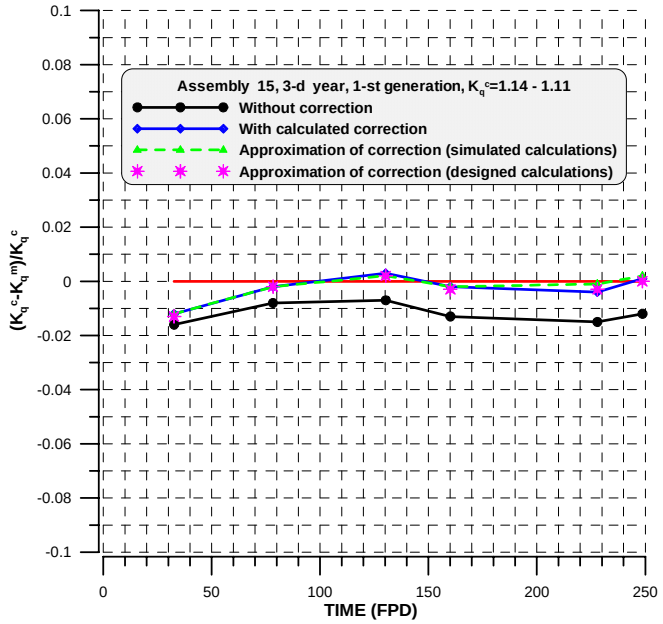

Fig. 4.11. Difference between calculated and measured relative assembly power during 20-th campaign. Assembly of the 1-st generation without Gd. Kola NPP Unit 3

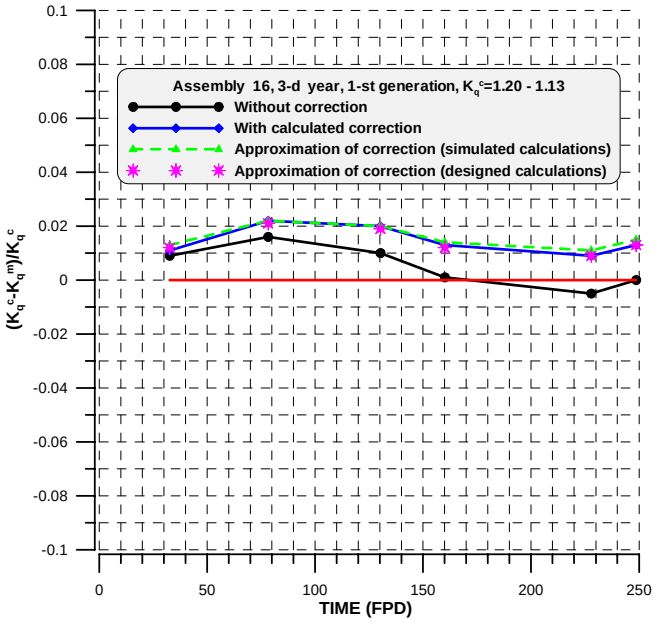

Fig. 4.12. Difference between calculated and measured relative assembly power during 20-th campaign. Assembly of the 1-st generation without Gd. Kola NPP Unit 3

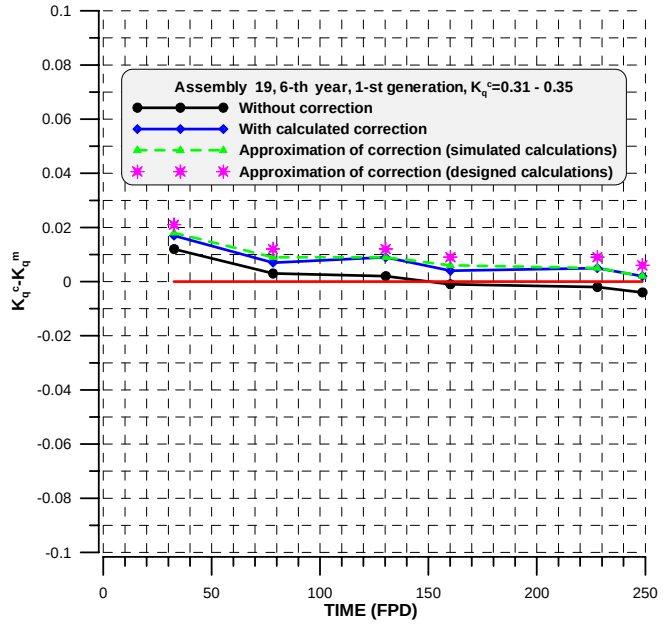

Fig. 4.13. Difference between calculated and measured relative assembly power during 20-th campaign. Assembly of the 1-st generation without Gd. Kola NPP Unit 3

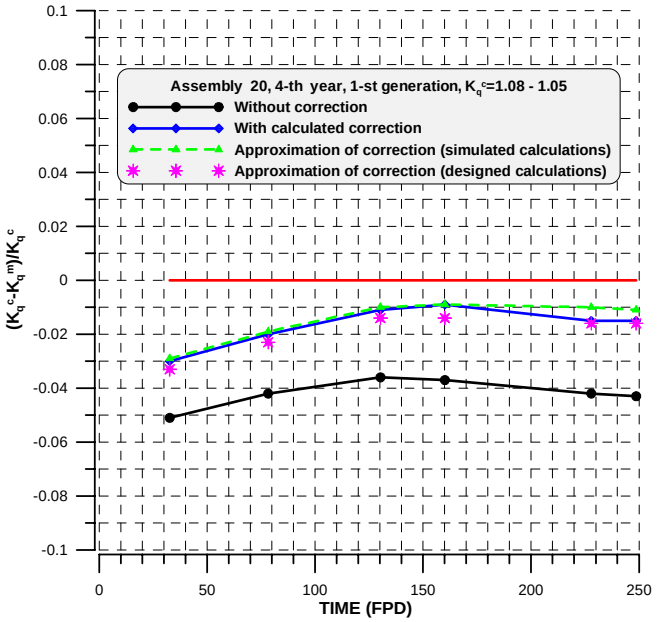

Fig. 4.14. Difference between calculated and measured relative assembly power during 20-th campaign. Assembly of the 1-st generation without Gd. Kola NPP Unit 3

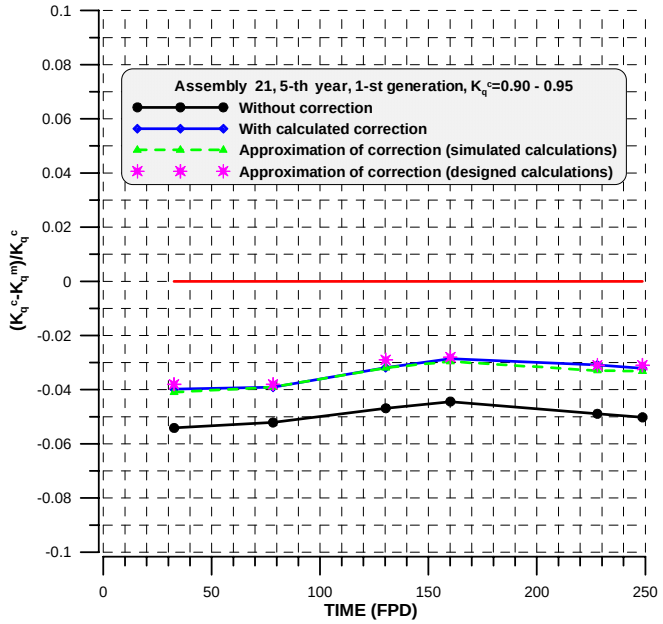

Fig. 4.15. Difference between calculated and measured relative assembly power during 20-th campaign. Assembly of the 1-st generation without Gd. Kola NPP Unit 3

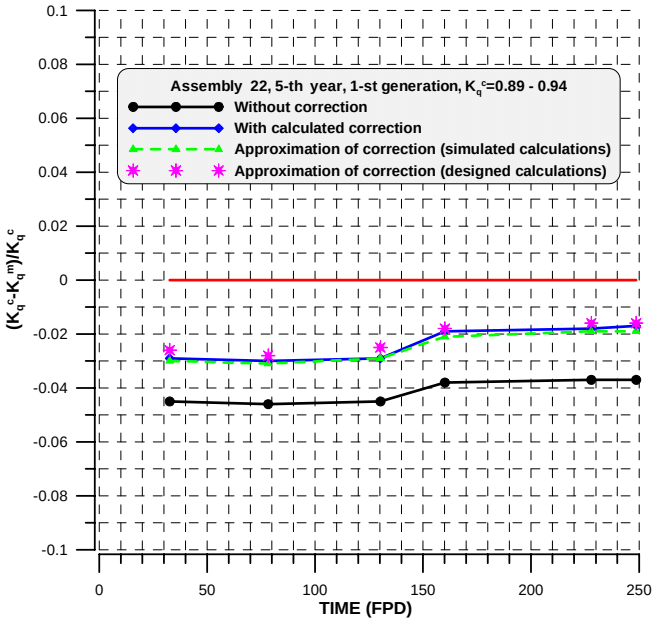

Fig. 4.16. Difference between calculated and measured relative assembly power during 20-th campaign. Assembly of the 1-st generation without Gd. Kola NPP Unit 3

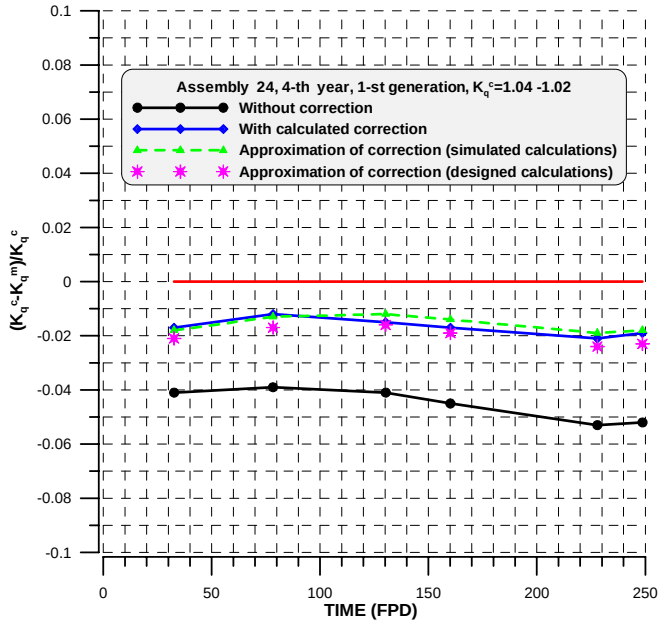

Fig. 4.17. Difference between calculated and measured relative assembly power during 20-th campaign. Assembly of the 1-st generation without Gd. Kola NPP Unit 3

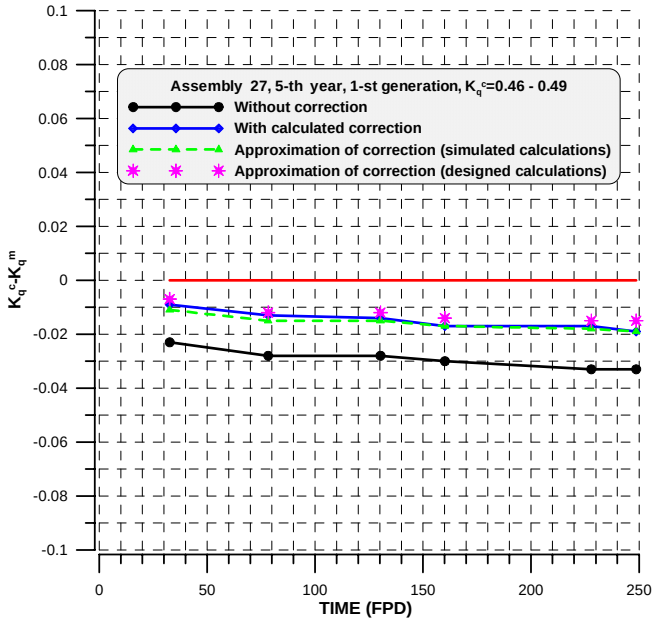

Fig. 4.18. Difference between calculated and measured relative assembly power during 20-th campaign. Assembly of the 1-st generation without Gd. Kola NPP Unit 3

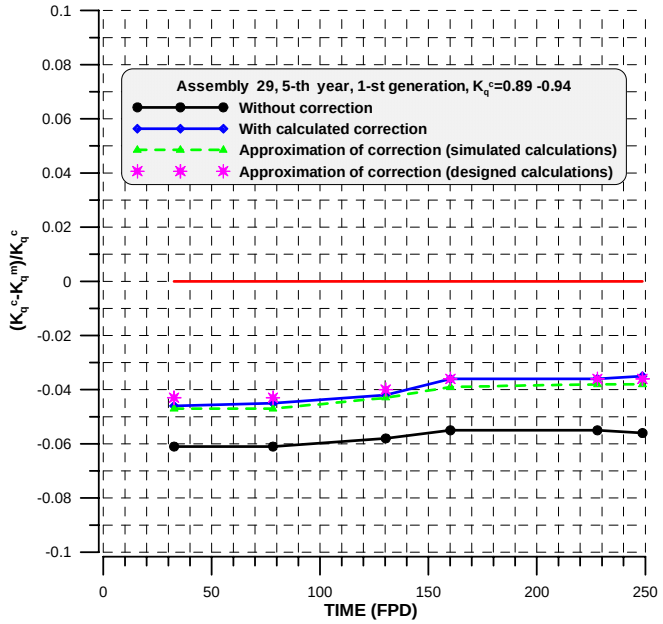

Fig. 4.19. Difference between calculated and measured relative assembly power during 20-th campaign. Assembly of the 1-st generation without Gd. Kola NPP Unit 3

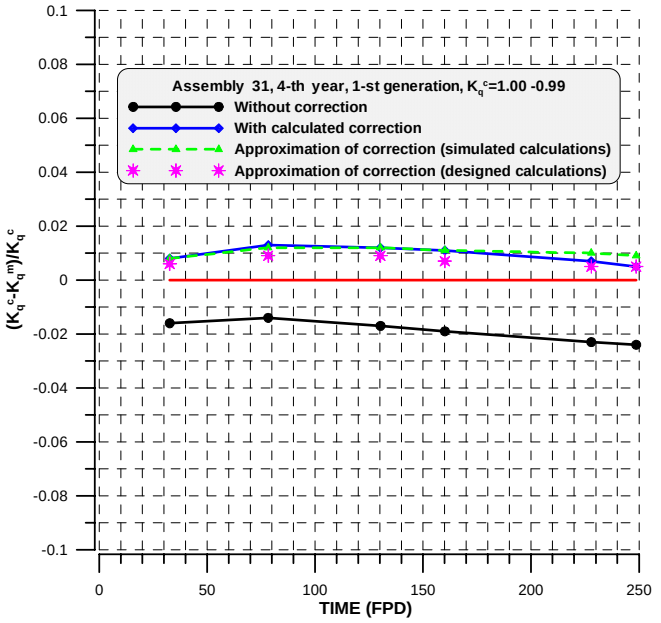

Fig. 4.20. Difference between calculated and measured relative assembly power during 20-th campaign. Assembly of the 1-st generation without Gd. Kola NPP Unit 3

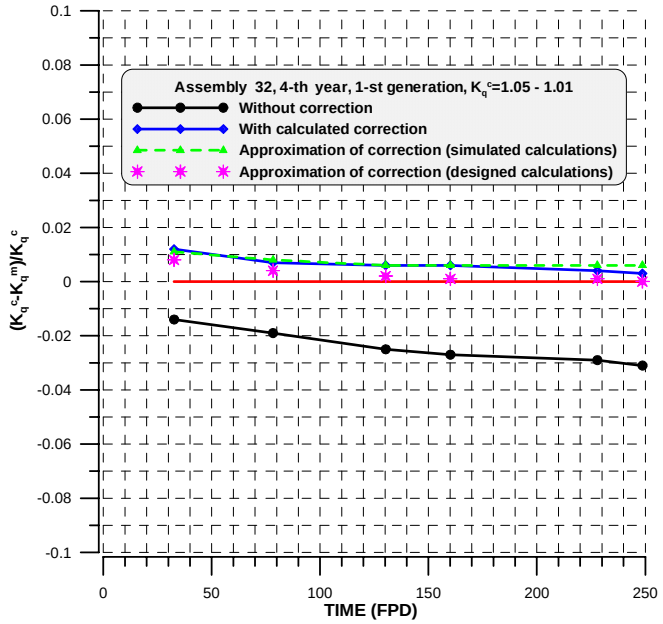

Fig. 4.21. Difference between calculated and measured relative assembly power during 20-th campaign. Assembly of the 1-st generation without Gd. Kola NPP Unit 3

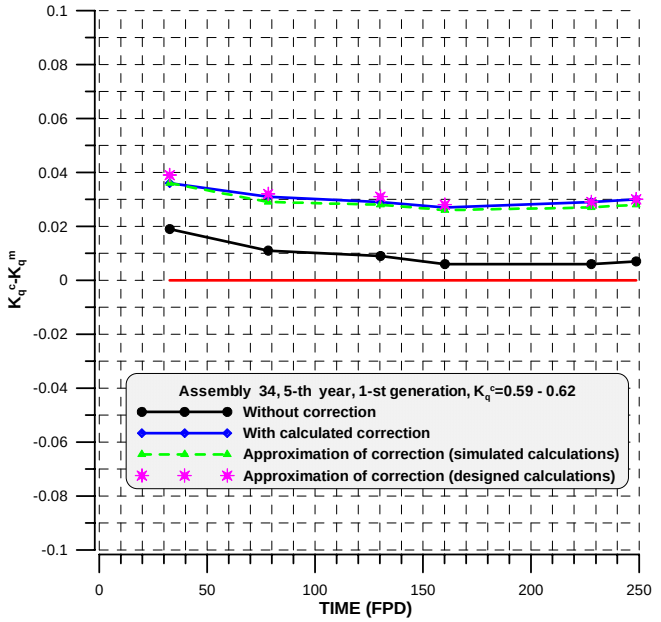

Fig. 4.22. Difference between calculated and measured relative assembly power during 20-th campaign. Assembly of the 1-st generation without Gd. Kola NPP Unit 3

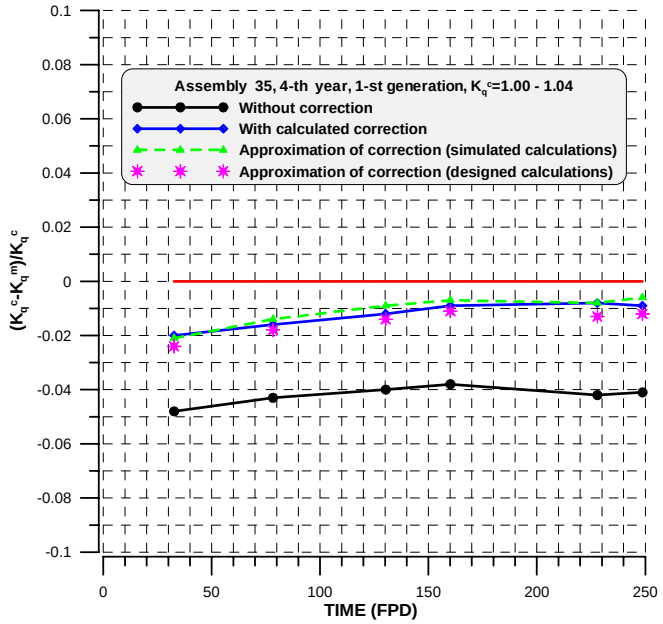

Fig. 4.23. Difference between calculated and measured relative assembly power during 20-th campaign. Assembly of the 1-st generation without Gd. Kola NPP Unit 3

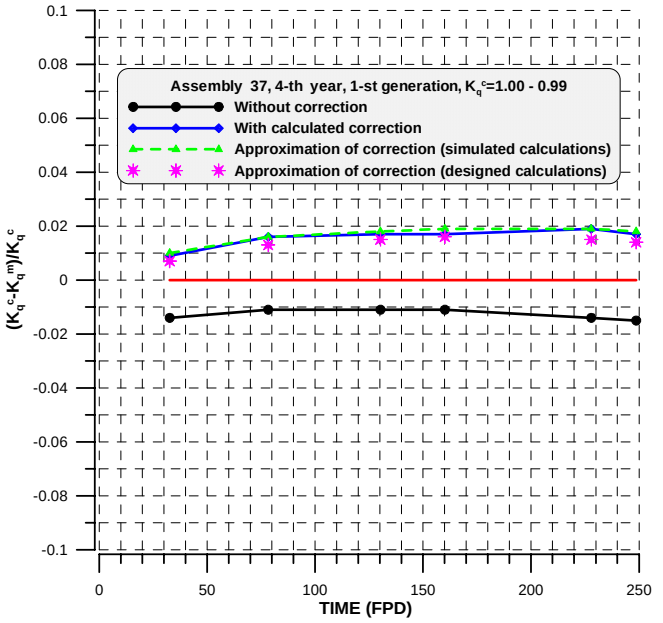

Fig. 4.24. Difference between calculated and measured relative assembly power during 20-th campaign. Assembly of the 1-st generation without Gd. Kola NPP Unit 3

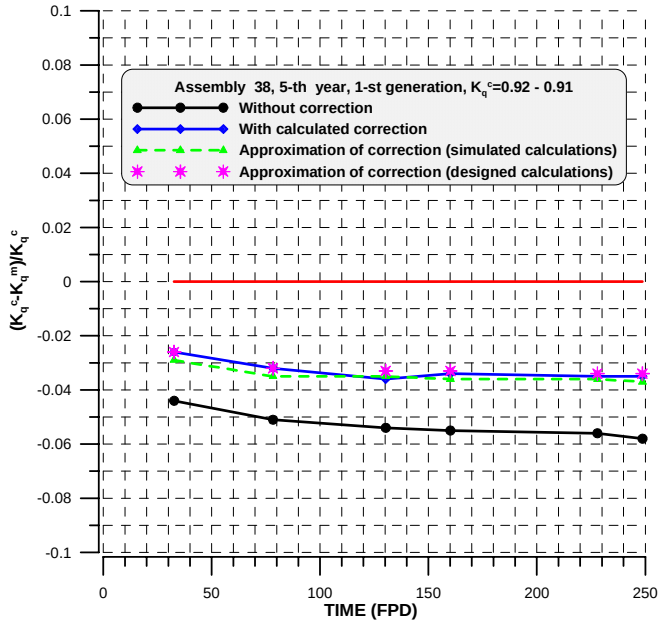

Fig. 4.25. Difference between calculated and measured relative assembly power during 20-th campaign. Assembly of the 1-st generation without Gd. Kola NPP Unit 3

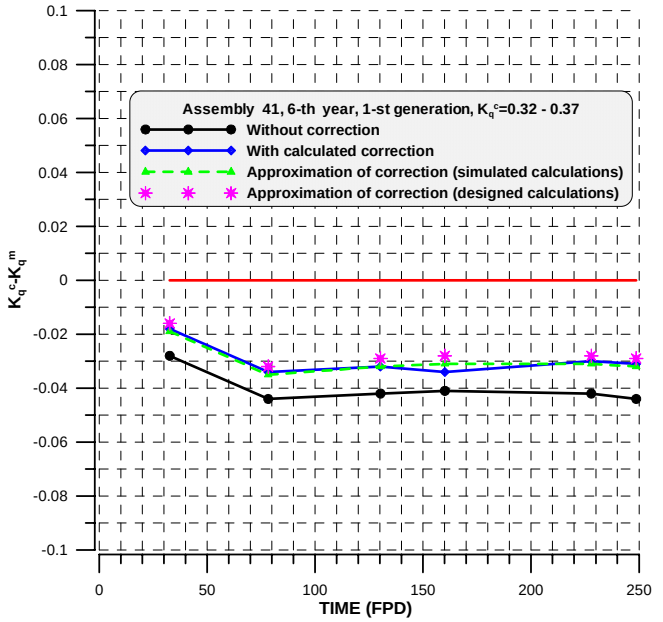

Fig. 4.26. Difference between calculated and measured relative assembly power during 20-th campaign. Assembly of the 1-st generation without Gd. Kola NPP Unit 3

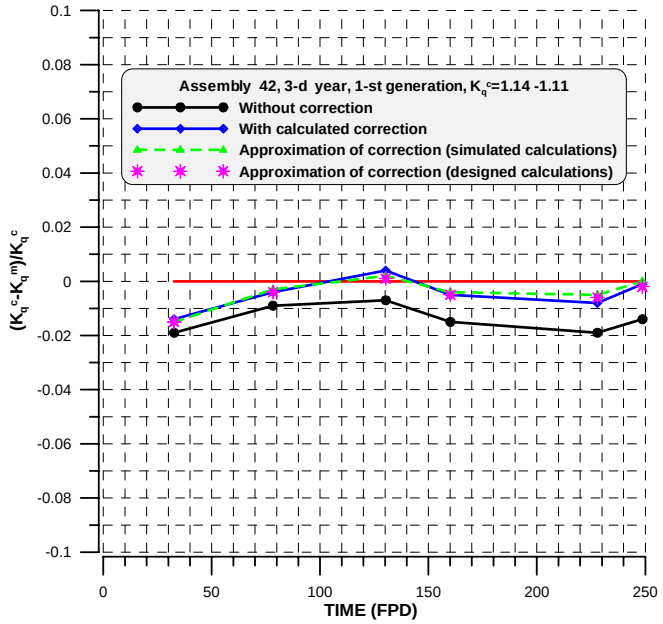

Fig. 4.27. Difference between calculated and measured relative assembly power during 20-th campaign. Assembly of the 1-st generation without Gd. Kola NPP Unit 3

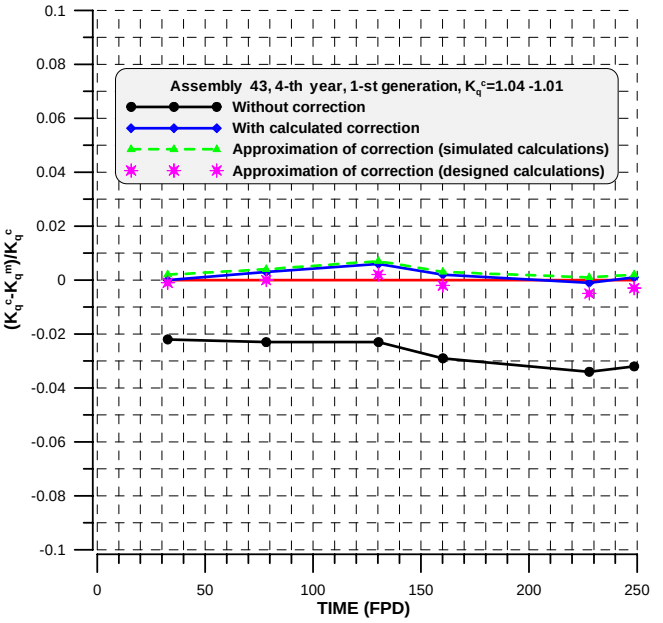

Fig. 4.28. Difference between calculated and measured relative assembly power during 20-th campaign. Assembly of the 1-st generation without Gd. Kola NPP Unit 3

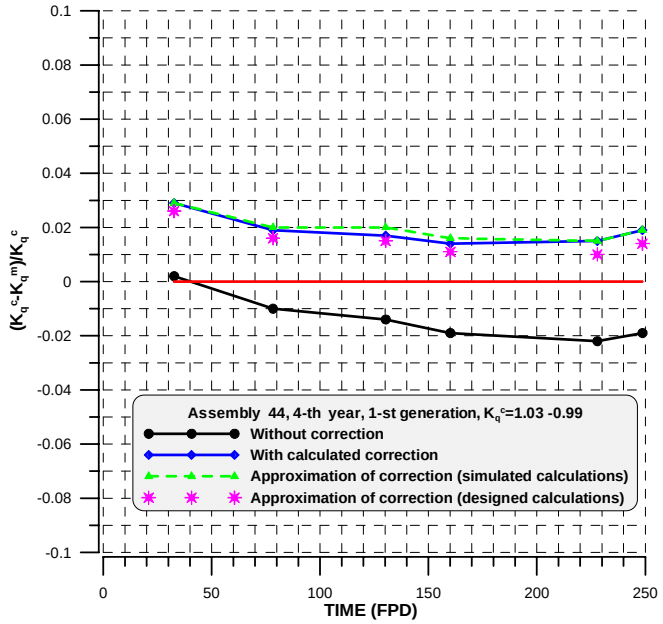

Fig. 4.29. Difference between calculated and measured relative assembly power during 20-th campaign. Assembly of the 1-st generation without Gd. Kola NPP Unit 3

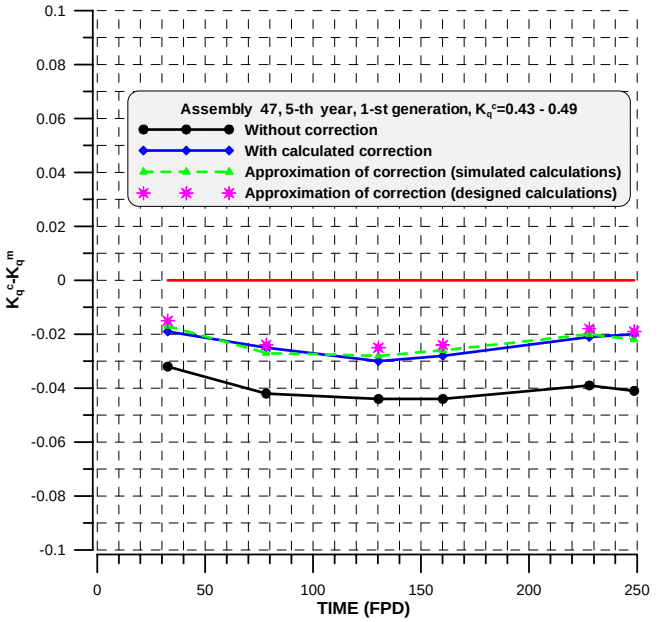

Fig. 4.30. Difference between calculated and measured relative assembly power during 20-th campaign. Assembly of the 1-st generation without Gd. Kola NPP Unit 3

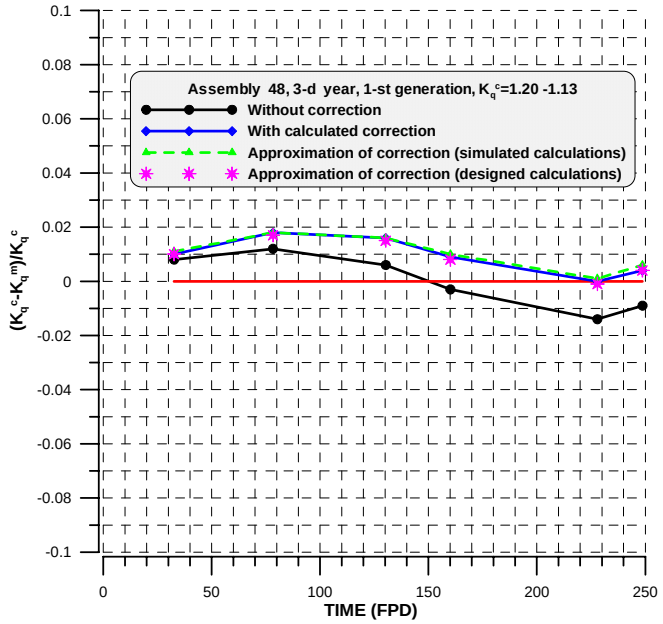

Fig. 4.31. Difference between calculated and measured relative assembly power during 20-th campaign. Assembly of the 1-st generation without Gd. Kola NPP Unit 3

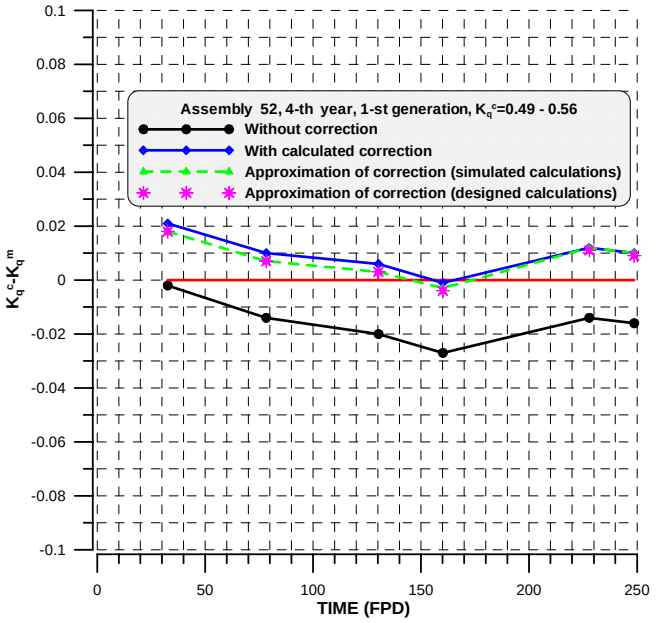

Fig. 4.32. Difference between calculated and measured relative assembly power during 20-th campaign. Assembly of the 1-st generation without Gd. Kola NPP Unit 3

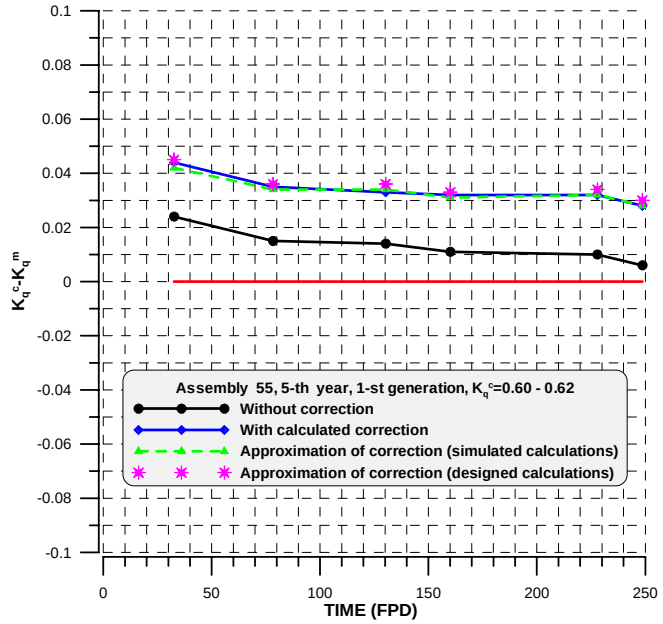

Fig. 4.33. Difference between calculated and measured relative assembly power during 20-th campaign. Assembly of the 1-st generation without Gd. Kola NPP Unit 3

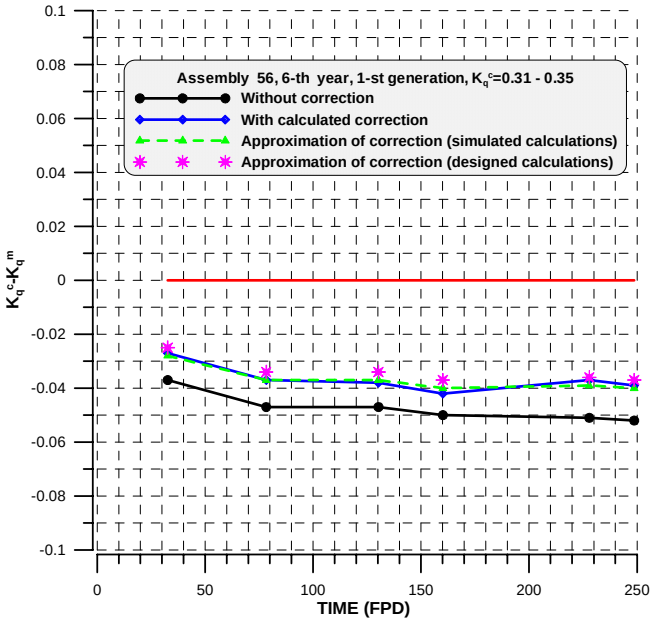

Fig. 4.34. Difference between calculated and measured relative assembly power during 20-th campaign. Assembly of the 1-st generation without Gd. Kola NPP Unit 3

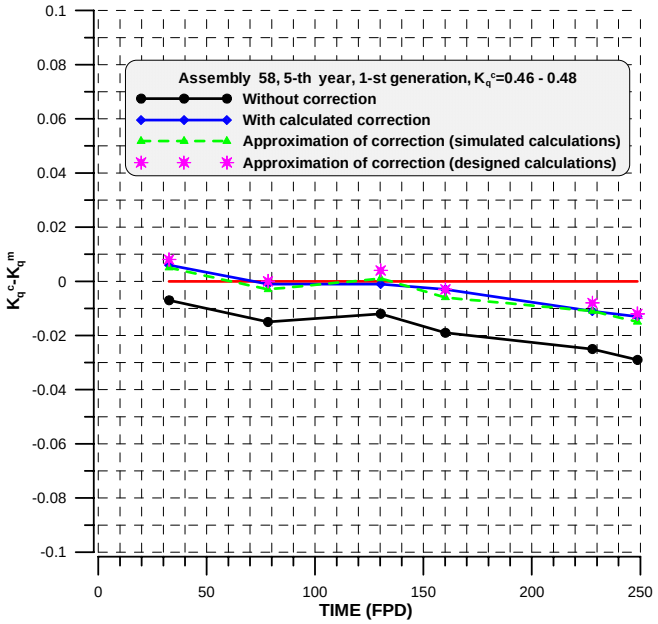

Fig. 4.35. Difference between calculated and measured relative assembly power during 20-th campaign. Assembly of the 1-st generation without Gd. Kola NPP Unit 3

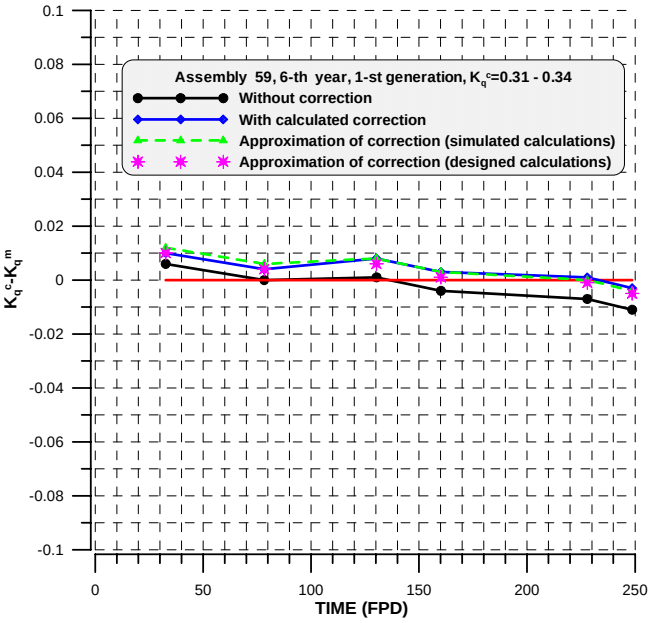

Fig. 4.36. Difference between calculated and measured relative assembly power during 20-th campaign. Assembly of the 1-st generation without Gd. Kola NPP Unit 3

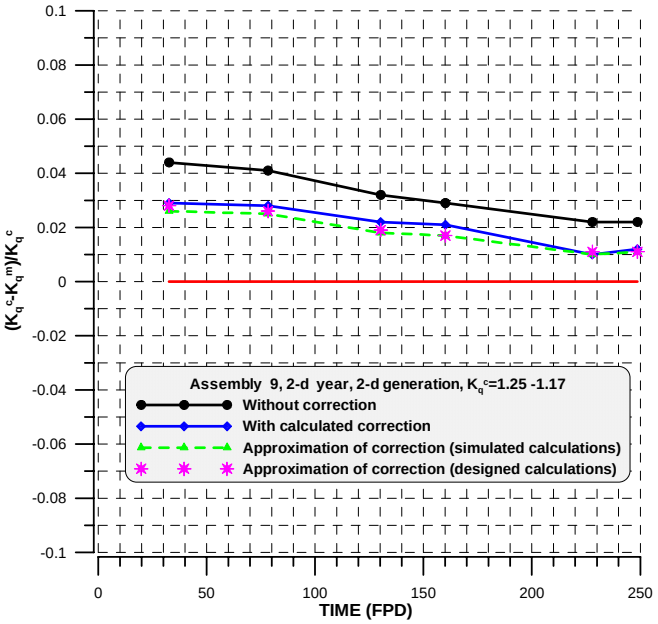

Fig. 4.37. Difference between calculated and measured relative assembly power during 20-th campaign. Assembly of the 2-nd generation with Gd-2. Kola NPP Unit 3

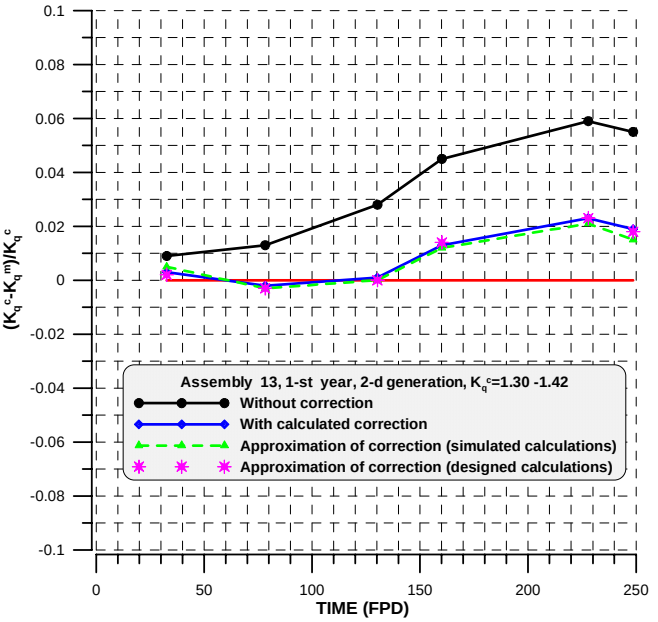

Fig. 4.38. Difference between calculated and measured relative assembly power during 20-th campaign. Assembly of the 2-nd generation with Gd-2. Kola NPP Unit 3

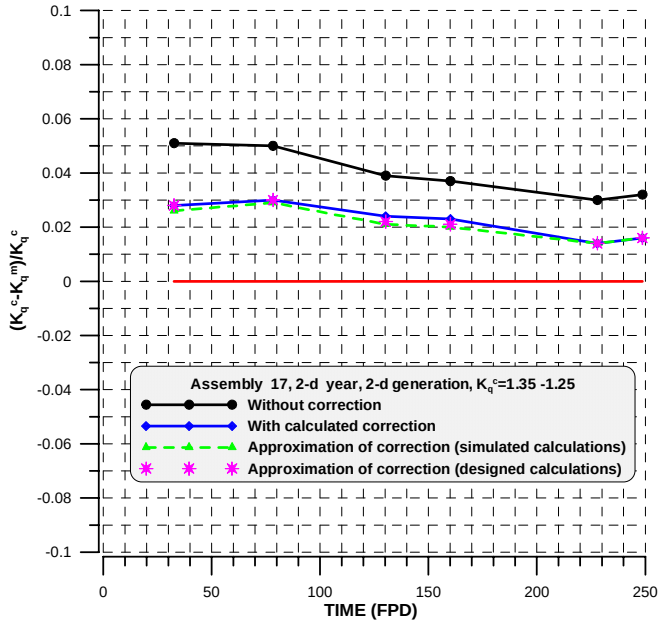

Fig. 4.39. Difference between calculated and measured relative assembly power during 20-th campaign. Assembly of the 2-nd generation with Gd-2. Kola NPP Unit 3

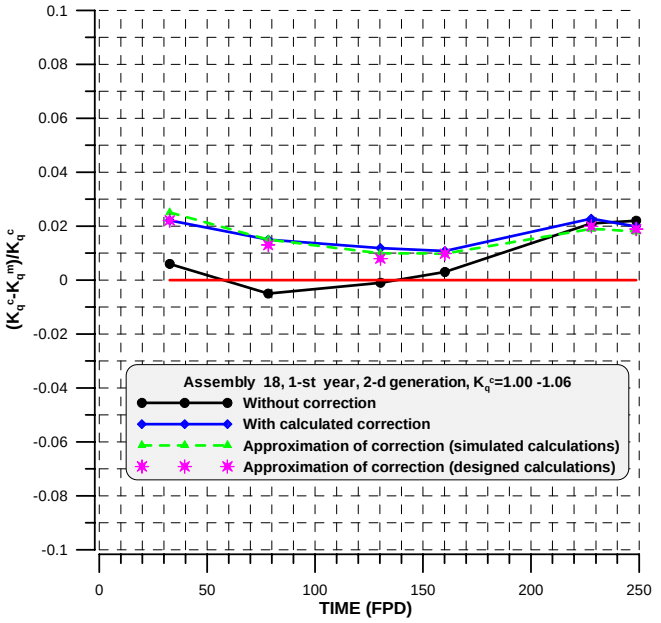

Fig. 4.40. Difference between calculated and measured relative assembly power during 20-th campaign. Assembly of the 2-nd generation with Gd-2. Kola NPP Unit 3

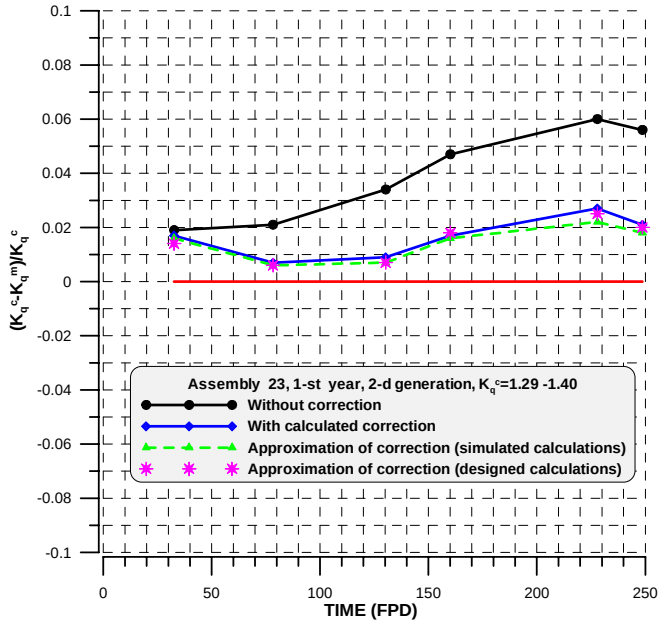

Fig. 4.41. Difference between calculated and measured relative assembly power during 20-th campaign. Assembly of the 2-nd generation with Gd-2. Kola NPP Unit 3

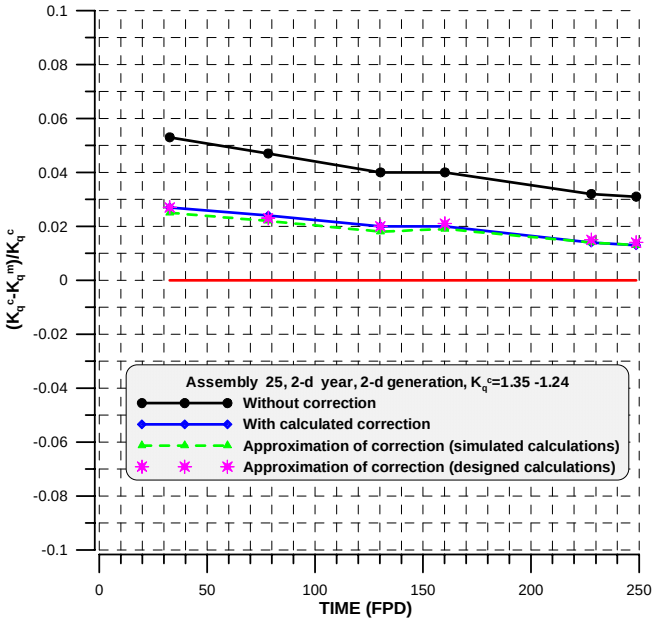

Fig. 4.42. Difference between calculated and measured relative assembly power during 20-th campaign. Assembly of the 2-nd generation with Gd-2. Kola NPP Unit 3

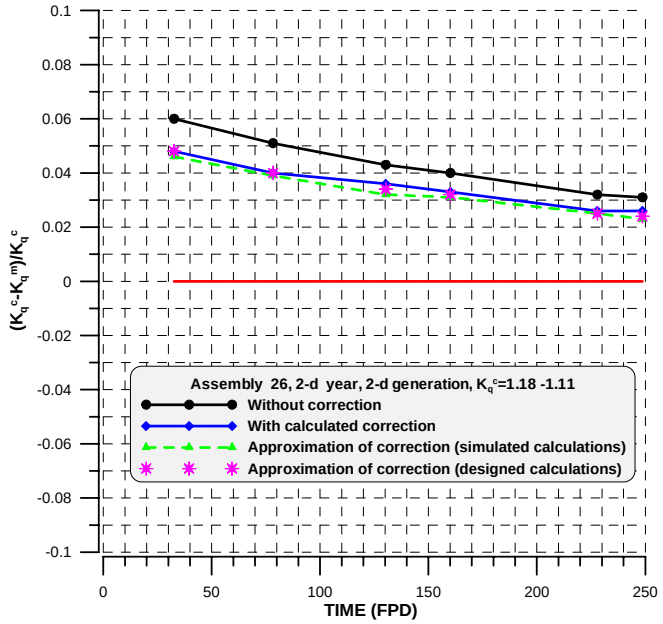

Fig. 4.43. Difference between calculated and measured relative assembly power during 20-th campaign. Assembly of the 2-nd generation with Gd-2. Kola NPP Unit 3

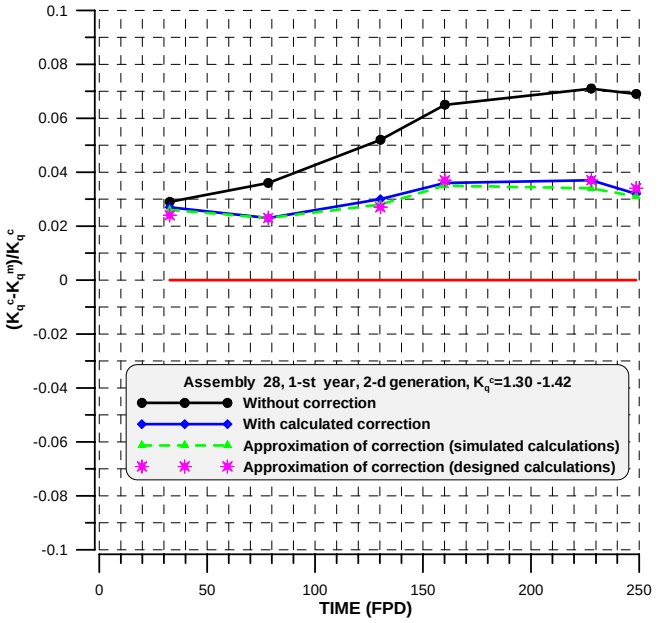

Fig. 4.44. Difference between calculated and measured relative assembly power during 20-th campaign. Assembly of the 2-nd generation with Gd-2. Kola NPP Unit 3

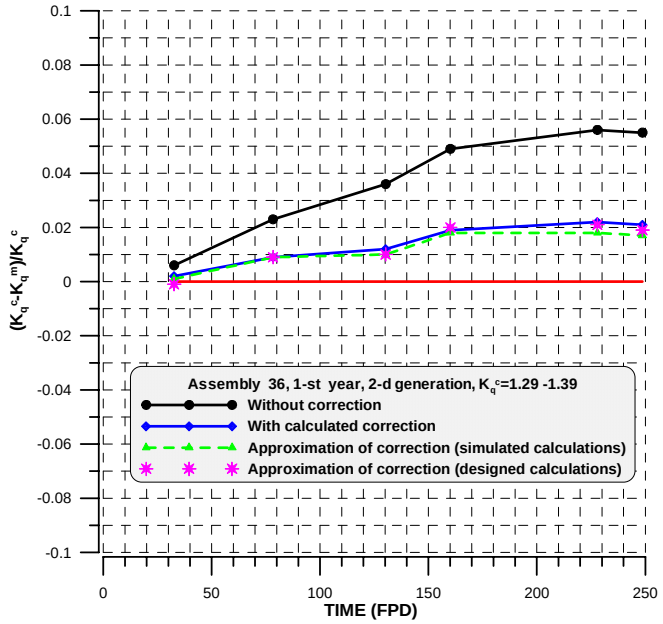

Fig. 4.45. Difference between calculated and measured relative assembly power during 20-th campaign. Assembly of the 2-nd generation with Gd-2. Kola NPP Unit 3

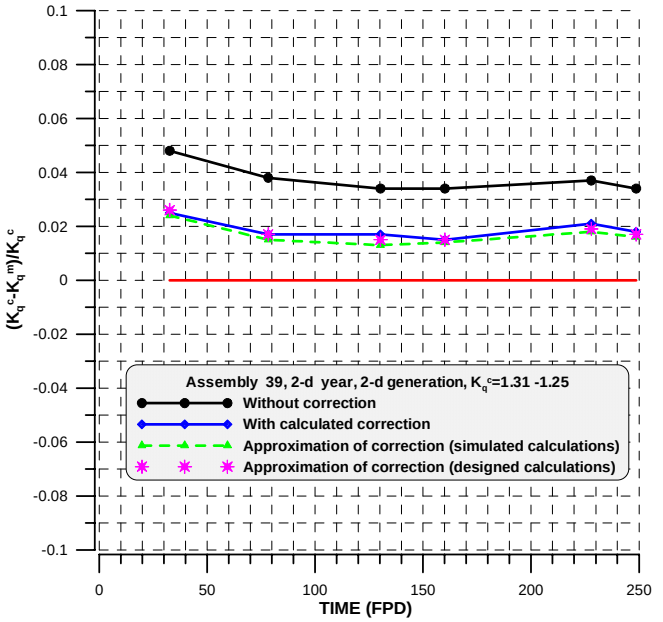

Fig. 4.46. Difference between calculated and measured relative assembly power during 20-th campaign. Assembly of the 2-nd generation with Gd-2. Kola NPP Unit 3

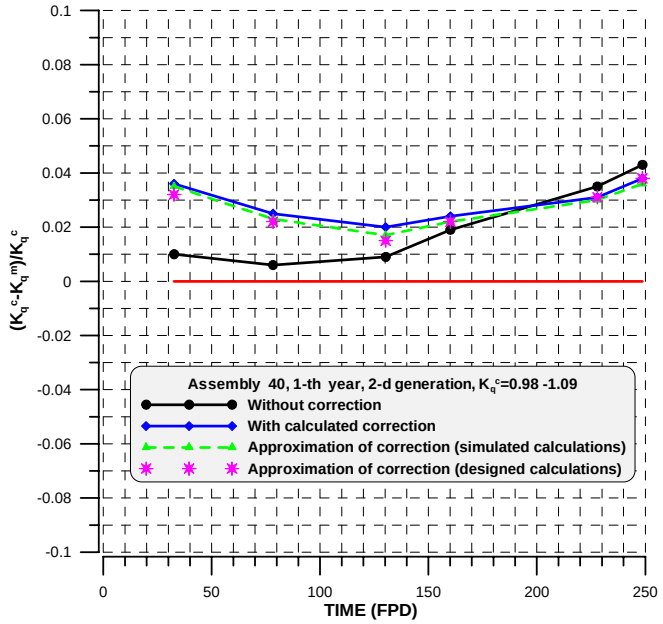

Fig. 4.47. Difference between calculated and measured relative assembly power during 20-th campaign. Assembly of the 2-nd generation with Gd-2. Kola NPP Unit 3

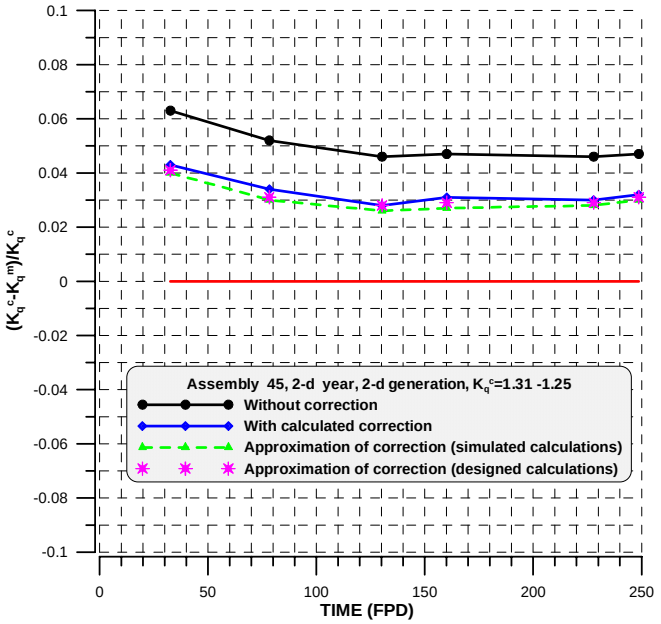

Fig. 4.48. Difference between calculated and measured relative assembly power during 20-th campaign. Assembly of the 2-nd generation with Gd-2. Kola NPP Unit 3

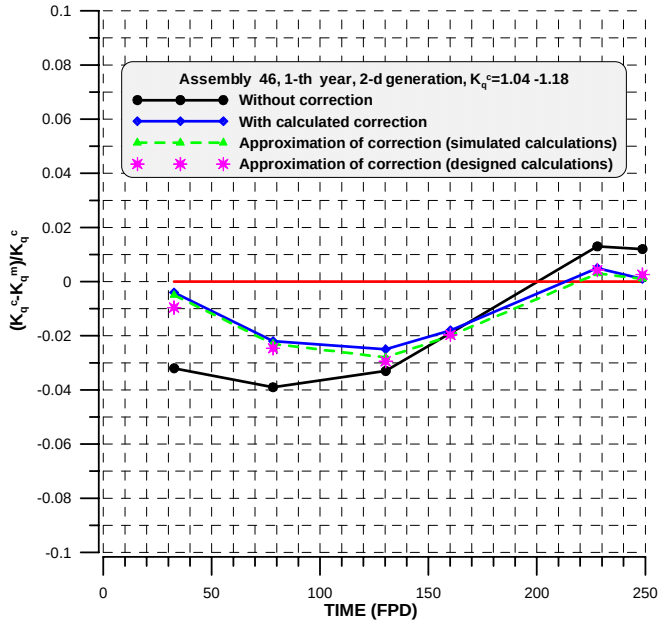

Fig. 4.49. Difference between calculated and measured relative assembly power during 20-th campaign. Assembly of the 2-nd generation with Gd-2. Kola NPP Unit 3

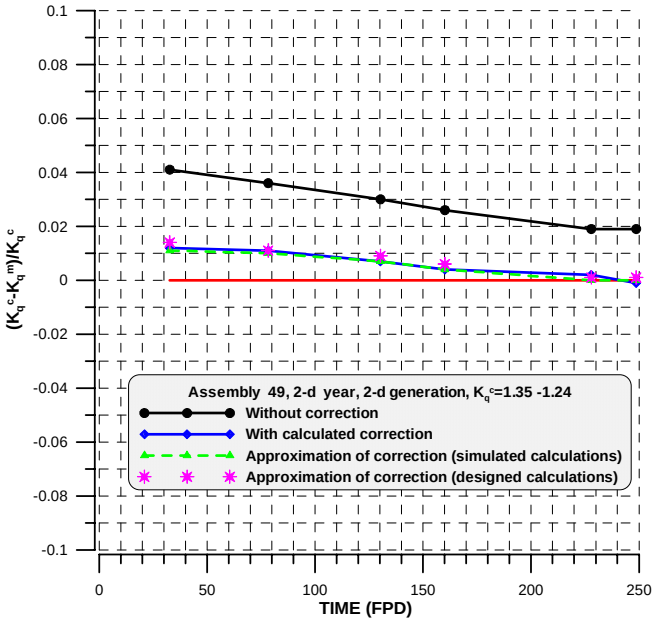

Fig. 4.50. Difference between calculated and measured relative assembly power during 20-th campaign. Assembly of the 2-nd generation with Gd-2. Kola NPP Unit 3

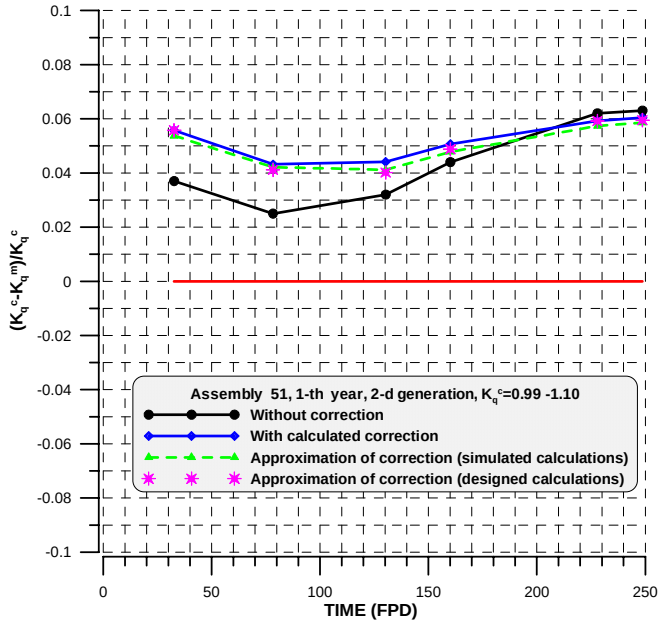

Fig. 4.51. Difference between calculated and measured relative assembly power during 20-th campaign. Assembly of the 2-nd generation with Gd-2. Kola NPP Unit 3

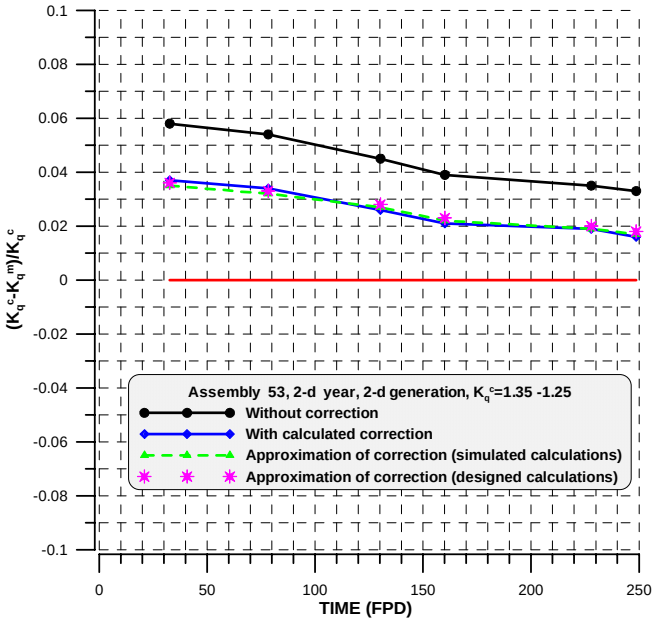

Fig. 4.52. Difference between calculated and measured relative assembly power during 20-th campaign. Assembly of the 2-nd generation with Gd-2. Kola NPP Unit 3

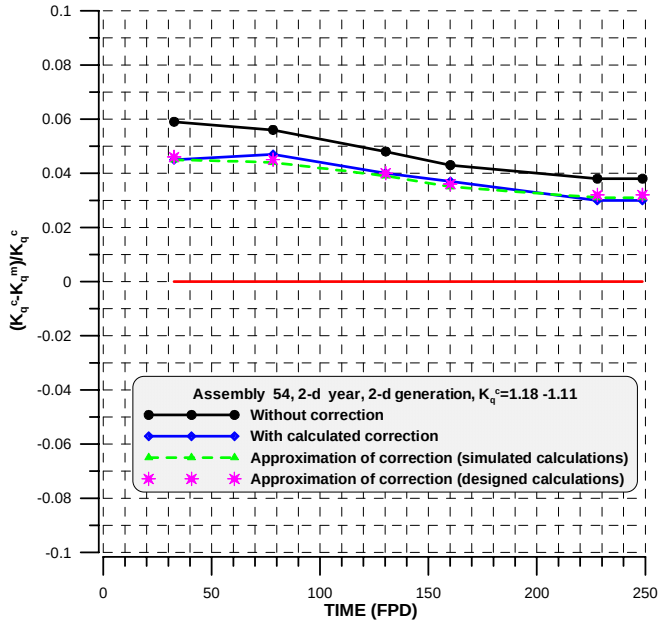

Fig. 4.53. Difference between calculated and measured relative assembly power during 20-th campaign. Assembly of the 2-nd generation with Gd-2. Kola NPP Unit 3

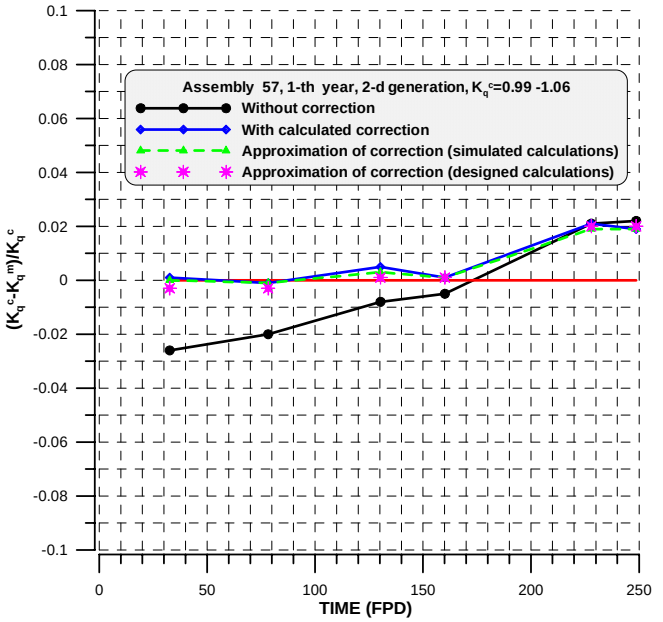

Fig. 4.54. Difference between calculated and measured relative assembly power during 20-th campaign. Assembly of the 2-nd generation with Gd-2. Kola NPP Unit 3